The University of Alberta
Printing Department
Edmonton, Alberta

THE UNIVERSITY OF ALBERTA

"CONTINUOUS, PRESTRESSED CONCRETE BEAMS WITH CONFINEMENT"

by

IAN H.G. DUNCAN

A THESIS

SUBMITTED TO THE FACULTY OF GRADUATE STUDIES

IN PARTIAL FULFILMENT OF THE REQUIREMENTS FOR THE DEGREE

OF MASTER OF SCIENCE

DEPARTMENT OF CIVIL ENGINEERING

EDMONTON, ALBERTA

FALL, 1969

UNIVERSITY OF ALBERTA

FACULTY OF GRADUATE STUDIES

The undersigned certify that they have read, and recommend to the Faculty of Graduate Studies for acceptance, a thesis entitled "CONTINUOUS, PRESTRESSED CONCRETE BEAMS WITH CONFINEMENT" submitted by IAN H.G. DUNCAN in partial fulfilment of the requirements for the degree of Master of Science.

ABSTRACT

The purpose of this series of tests was to investigate the effect of continuity on prestressed concrete beams with confined compression zones. Previous tests on beams with similar sections, though simply supported, have provided substantial evidence of the increase in deformation capacity of prestressed concrete beams with this additional reinforcement. This series set out to expose any limitations in the use of continuous beams reinforced in this manner, and to investigate the distribution of moments at load increments up to failure.

Six beams were tested, each continuous over two spans and loaded at each mid-span. The primary variables were span, degree of reinforcement and presence of confinement.

Measurements of reactions, change and distribution of strain, and deflection were taken at every load increment. The results of the tests are presented in terms of both measured and derived loads and deformations.

Over-reinforced beams failed in tension at higher ultimate moments than would be expected without confinement, and with considerably more ductility. However, the presence of confinement made little difference to the behaviour and failure modes of the under-reinforced beams.

Full redistribution of moments was not required to achieve the ultimate moments at the critical sections, though variable amounts

of redistribution were developed. In all cases, failure was diverted from the interior support, where it would be expected, to one of the spans. Reasons for this inconsistency, as well as recommendations for future tests, are proposed.

ACKNOWLEDGEMENTS

The Author wishes to thank:-

Professor J. Warwaruk for his guidance,

Mr. M.K. Wilkinson for his assistance,

Mr. H. Panse and his staff for their help and co-operation and,

Mrs. Jan Theriault for her patience while typing the manuscript.

Funds and facilities for the experimental work were made available by the Department of Civil Engineering, and by the National Research Council through Grant NRC A1696. The Canadian Commonwealth Scholarship and Fellowship Committee provided financial support.

TABLE OF CONTENTS

Table of Contents

Appendices

LIST OF TABLES

LIST OF FIGURES

CHAPTER I

INTRODUCTION

The application of limit design to any type of structure requires that the material possesses sufficient ductility to permit the necessary inelastic rotations to occur. Structural steel members usually exhibit adequate rotation capacity to permit full redistribution of moments to adjacent parts of an indeterminate structure before failure. On the other hand, the rotation capacity of reinforced concrete members is restricted by the limited strain which can be achieved in the concrete before failure. In general, for relatively small amounts of reinforcement, the available ductility in a reinforced concrete section depends on the inelastic characteristics of the steel, whilst sections with a high reinforcement ratio exhibit very little, if any, ductility before failure.

These aspects become more important with prestressed concrete sections for two principal reasons:- The high-grade steel, which is used in the fabrication of prestressed concrete members, displays particularly poor inelastic properties, with an ultimate strain often as little as one third that of common reinforcing steel. Secondly, the steel loses a fraction of its limited ductility during the prestressing operation. Therefore, although the required ultimate moment of a section may be reached, the member may not posses sufficient rotation capacity to permit a limit design method to be safely used.

For these reasons, attention has been directed recently, by many investigators,to the possibility of providing ductility in a reinforced concrete section by improving the inelastic characteristics of the compressed concrete, which, by itself, usually exhibits limited deformation before failure. One way of achieving this improvement is to confine the concrete by means of spiral reinforcement. It is well established that the deformation characteristics of columns are improved using this same principle.

Previous tests, on simply supported beams, have indicated that, by including confinement in an over-reinforced, prestressed concrete section, both improved moment capacity and deformation characteristics have been achieved. This present test series is the first in the University of Alberta programme to investigate the behaviour of confined, continuous prestressed concrete beams. One of the objects of the series was to investigate any inconsistencies in the application of results from earlier tests on simply supported beams to continuous beams.

Six beams were tested. The main variables were span, degree of reinforcement and presence of confinement, although small variations in effective prestress and concrete strength were unavoidable.

The beams were tested in combined flexure and shear, though the flexural behaviour was the main subject for investigation. The results are presented in terms of applied load and resulting deformations, with particular reference to the effect of continuity.

CHAPTER II

REVIEW OF PREVIOUS TESTS

2.1 Confined Concrete

The use of spiral reinforcement as a means of improving the deformation characteristics of compressed concrete is relatively recent in the context of flexural members. However, spiral reinforcement has been used in the design of columns for many years. It is well established that the failure of a column so reinforced is more ductile than a column without confinement, and a reserve of strength is often achieved.

The use of spiral reinforcement in beams has been studied by several investigators. Base and Read[2] tested both reinforced and prestressed concrete beams with confinement; their conclusions may be summarized as follows:-

(a) Rectangular, prestressed beams are particularly lacking in plasticity at failure. Helical binding is an economical and effective way of producing satisfactory plastic failure characteristics.

(b) Reinforced concrete beams with a balanced steel ratio fail in a brittle manner unless the compressed concrete in the region of the plastic hinge is bound. Helical binding transforms the brittle flexural failure into the ideal plastic failure with the hinge moment of resistance nearly constant for a large rotation.

(c) In over-reinforced beams, the effect of helical binding is to increase the maximum moment of resistance of the plastic hinge to a value significantly higher than a similar beam without binding.

Base and Read noted that, for the prestressed beams, there was a considerable discrepancy between the observed and estimated ultimate moments. They believed that this might be due to two causes:- In beams where failure is primarily due to crushing of the concrete, the triaxial state of compression that exists under the loading plates is known to result in an increased moment of resistance at these locations. This produces an increase in the failing load of beams loaded at a single point, and this increase is influenced by the span of the beam; the shorter the span, the greater the increase. Their second observation was that in prestressed beams, the fact that the compression zone moves down from the top of the beam at the loaded section towards the bottom of the beam at the negative moment region appears to result in an additional confining effect in the compression zone of short beams under single point loading.

All the beams tested by Base and Read were simply supported, and loaded at mid-span.

2.2 Simply-supported, prestressed concrete beams with confinement.

The effect of confining the compression zone in prestressed concrete beams on their deformation characteristics has been the subject of two recent investigations at the University of Alberta.

Ward[3] tested twelve beams with a constant moment region, thus inducing a state of pure flexure. The tests indicated that the presence

of confinement, even prior to spalling, influenced the load-deformation relationships. Ward's main conclusions were:-

(a) The use of spiral confinement in the compression zone was found to be very effective in producing ductile failures in beams which under normal conditions were over-reinforced.

(b) The ultimate moment and curvature for beams with large amounts of confinement were dependent mainly on the amount of tension reinforcement and only slightly on the concrete strength.

Wilkinson[4] tested twelve beams in combined flexure and shear, with varying spiral pitch, degree of reinforcement and span. He concluded:-

(a) that for similar concrete strengths, amount of tension reinforcement and span length; to ensure tension failures in prestressed concrete beams which have large amounts of tension reinforcement the degree of confinement must be sufficient so that yield strains are developed in the tension reinforcement.

(b) that for similar concrete strengths, amount of tension reinforcement and degree of confinement; a change in the failure mode due to a reduced span length depended on the shear resistance of the beam. If the concrete strength and web reinforcement were sufficient to develop the required shear resistance, then the failure mode depended on the amount of confinement.

(c) that for similar concrete strengths, degree of confinement and span length; a larger amount of tension reinforcement did not significantly affect the behaviour and ultimate curvature, however it did increase the resisting moment capacity.

Wilkinson used 1", 2" and 3" pitches for the spiral reinforcement. He commented that the 1" and 2" pitches were effective in confining the concrete, though in some instances the 3" pitch was not adequate.

2.3 Unconfined, continuous prestressed concrete beams

Hawkins, Sozen and Siess[5] conducted an extensive study into the behaviour of continuous, prestressed concrete beams, without confinement. They were concerned both with shear and flexural behaviour. However, of particular relevance are their results with regard to moment redistribution. One of their major variables was the ratio of the effective depth, and hence moment capacity, at mid-span and interior support sections. Those beams whose effective depths at the centre were less than those at mid-span displayed significant moment redistribution after cracking, as illustrated on a load-moment plot. Those beams whose effective depths at the centre were greater than or equal to those at mid-span displayed very little, if any, redistribution. Three of their beams, from the latter category, displayed erratic behaviour on the load-moment plot, in fact the span moments remained greater than the support moments up to failure.

CHAPTER III

PRESENT TEST SERIES

The present test series forms one part of an overall programme being conducted at the University of Alberta to investigate the flexural behaviour of prestressed concrete beams with confinement. It was mainly concerned with the distribution of moments in continuous beams, and with the effect of confining the compression zone on the internal rotations of continuous prestressed concrete beams.

Six beams were tested; three were continuous over two 10' spans, and three were continuous over two 5' spans. Each set of three beams included two with a nominally balanced reinforcement ratio. One of these two included spiral reinforcement; the other did not, so as to provide a control test. The third of each set of three was nominally over-reinforced, and included spiral reinforcement. The beams were designated as follows:-

H.108	H.106	H.106.C	
J.58	J.56	J.56.C	where the figures:-

(8 or 6) refer to the NUMBER OF 5/16" STRANDS in the section;

(5 or 10) refer to the SPAN LENGTH in FEET; and

'C' refers to the CONTROL beam in each set, being the beam without spiral reinforcement.

The test beam sections and elevations are shown in Figures 3.1, 3.2 and 3.3.

Each beam was designed so that the three critical sections had the same moment capacity, though a spiral pitch of 1" was used over the interior support, whereas in the mid-span regions a 2" pitch was used.

All preliminary calculations for the design of the sections were based on a concrete cylinder strength of 5000 p.s.i. and an effective prestress of 135 k.s.i. Any difference between the ultimate moments of the sections with 1" and 2" spiral pitches was not taken into account for these preliminary calculations.

The shear reinforcement was designed in accordance with the A.C.I. Standard (318-63)[1], including the capacity reduction factor. The ultimate shear forces were calculated assuming full redistribution of moments.

The effect of secondary moments, due to the restraint normally imposed on a continuous beam by intermediate supports, was overcome by ensuring that each beam was "seated" on its three supports at the beginning of each test. To achieve this condition, the relative height of the exterior and interior supports was adjusted both by packing and then by seating the beam on a Plaster of Paris bed. This allowed the beam to be supported regardless of any initial deflections due to primary moments caused by the prestressing force.

The beams were loaded by applying equal point loads at the centre of each span. A steel plate distributed the load from each jack into the beam. Sufficient load increments were applied so that the behaviour after cracking could be well recorded.

The beam variables are all presented in Table 3.1. The effective prestress, after losses, is equal to the horizontal component of the tensions in the strands, derived as outlined in Section A.3. The concrete strengths are those representing the average of three cylinder compression tests per batch. The parameter (p.fsu./f'c) provides an indication of the degree of reinforcement in the section; the A.C.I. Code limit on this quantity is 0.3.[1]

Figure 3.4 shows details of the instrumentation of the beams for testing. Reactions were derived from the readings of the electrical strain-gages attached to each 100 kip. load-cell. An accuracy of $\pm$ 0.1 kip. was achieved for these readings. Deflections were measured by dial-gages, reading to 0.001", and also by a survey level reading onto scales graduated to 0.01". Figure 3.5 illustrates the method by which the dial-gages and scales were attached to the beam. The studs, for the mechanical strain-gages, were fixed to one face of each beam using sealing-wax. The 10" gage lengths were for use with a Whittemore strain-gage, and the 8" gage lengths were for use with a Demec strain gage.

Figure 3.6 shows beam J56 ready for testing. The profile of the prestressing strands, as shown in Figure 3.6, was drawn on the surface of each beam to facilitate the interpretation of photographs which were taken during the tests to provide a record of the cracking behaviour.

TABLE 3.1

DETAILS OF THE TEST BEAMS

	SOUTH				CENTRE				NORTH			
BEAM	P_e (k.s.i.)	f'_c (p.s.i.)	$\frac{p.f_{su}}{f'_c}$	Spiral Pitch	P_e (k.s.i.)	f'_c (p.s.i.)	$\frac{p.f_{su}}{f'_c}$	Spiral Pitch	P_e (k.s.i.)	f'_c (p.s.i.)	$\frac{p.f_{su}}{f'_c}$	Spiral Pitch
H108	124	4960	0.432	2"	122	5160	0.415	1"	124	5140	0.417	2"
H106	121	5960	0.270	2"	116	5640	0.286	1"	121	5820	0.276	2"
H106.C	120	4600	0.349	-	119	5440	0.296	-	120	5560	0.288	-
J58	141	5670	0.376	2"	132	5890	0.366	1"	141	6110	0.349	2"
J56	151	6060	0.265	2"	143	5690	0.282	1"	151	5330	0.302	2"
J56.C	143	5700	0.282	-	138	5500	0.291	-	143	5300	0.305	-

N.B. $A_{s\ (6)} = .348 \quad (\rho_{(6)} = .058)$

$A_{s\ (8)} = .464 \quad (\rho_{(8)} = .077)$

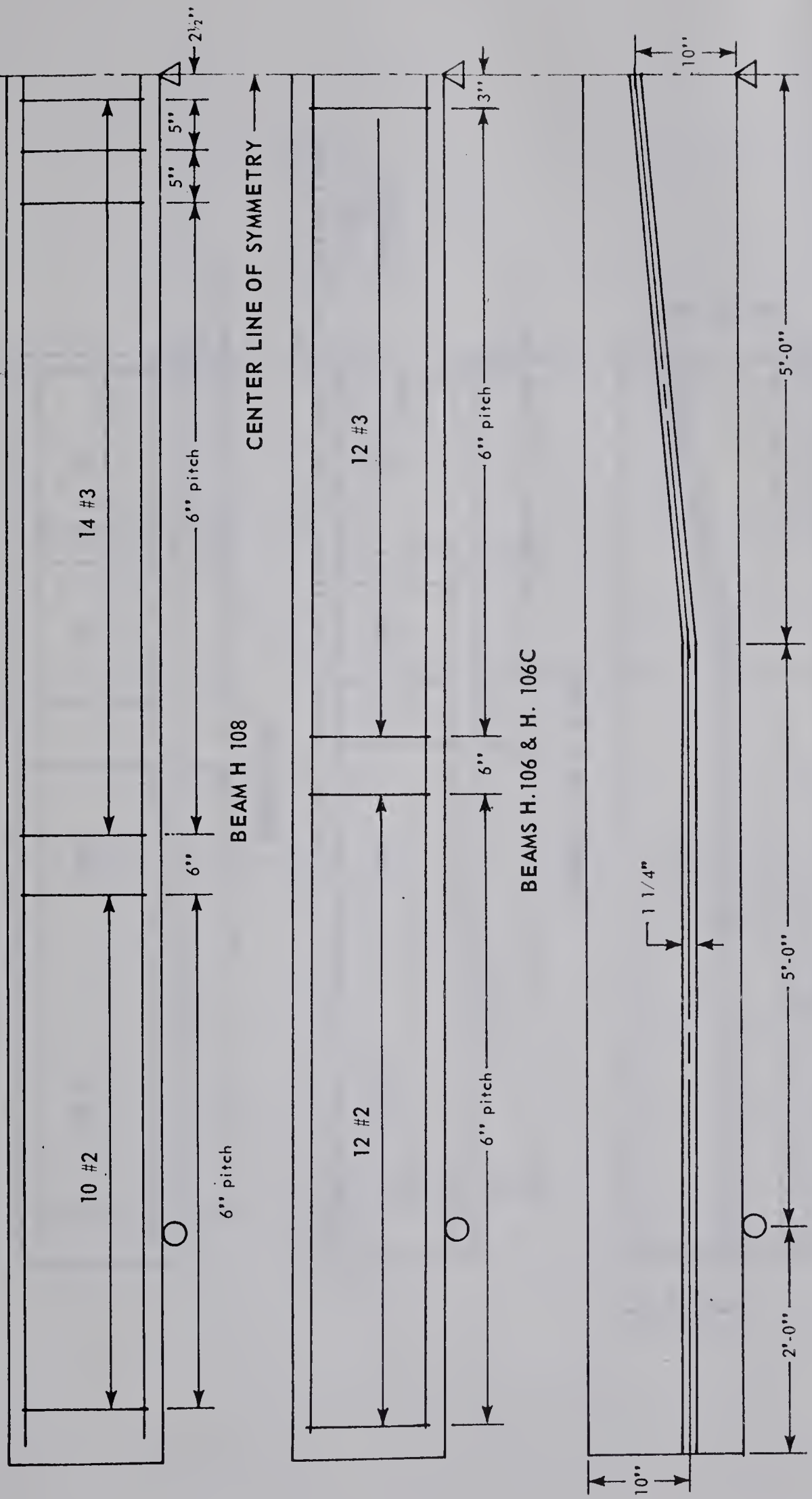

FIGURE 3.1 SHEAR REINFORCEMENT AND STRAND PROFILE FOR SERIES "H" BEAMS

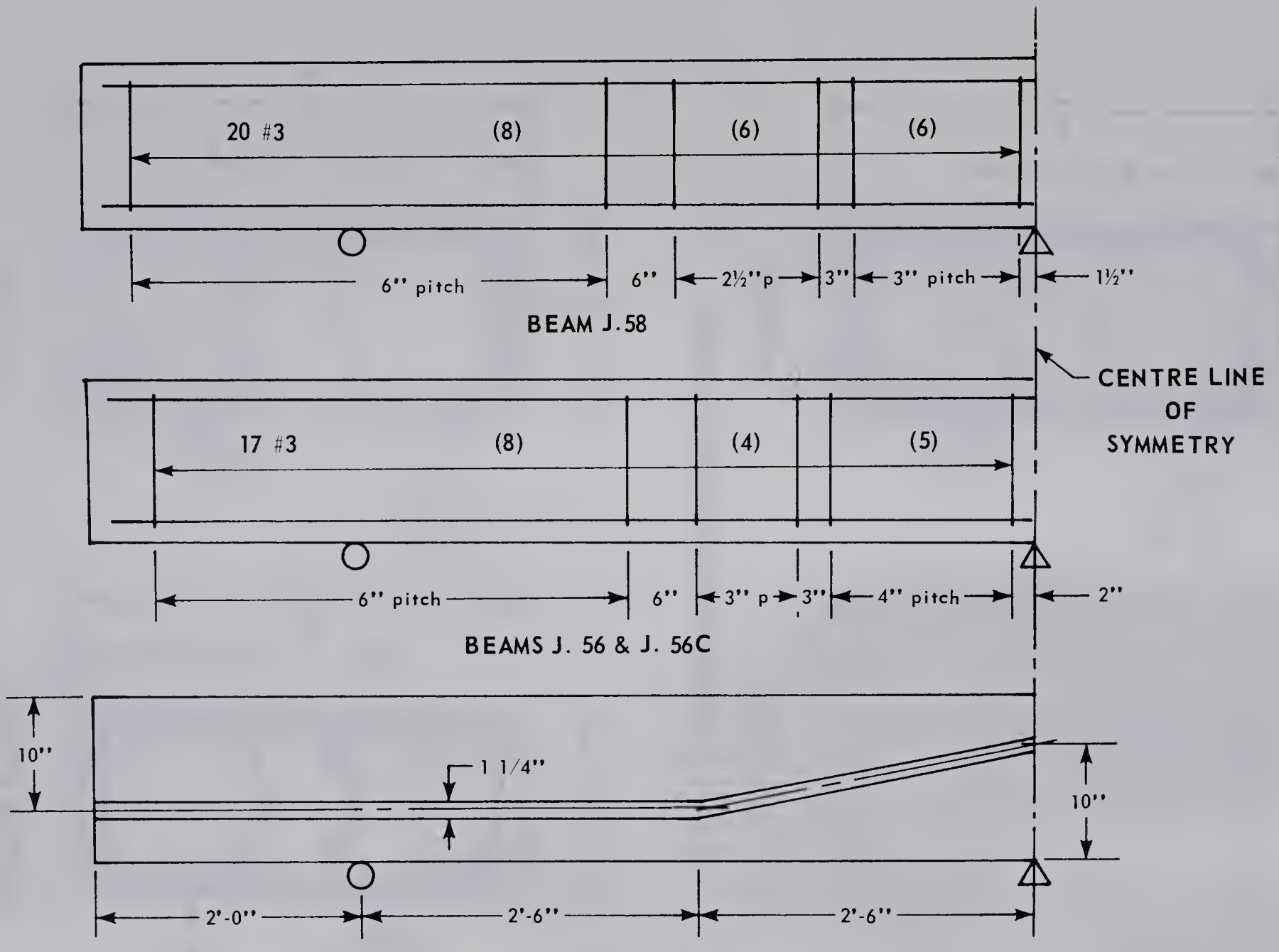

FIGURE 3.2 SHEAR REINFORCEMENT AND STRAND PROFILE FOR SERIES "J" BEAMS

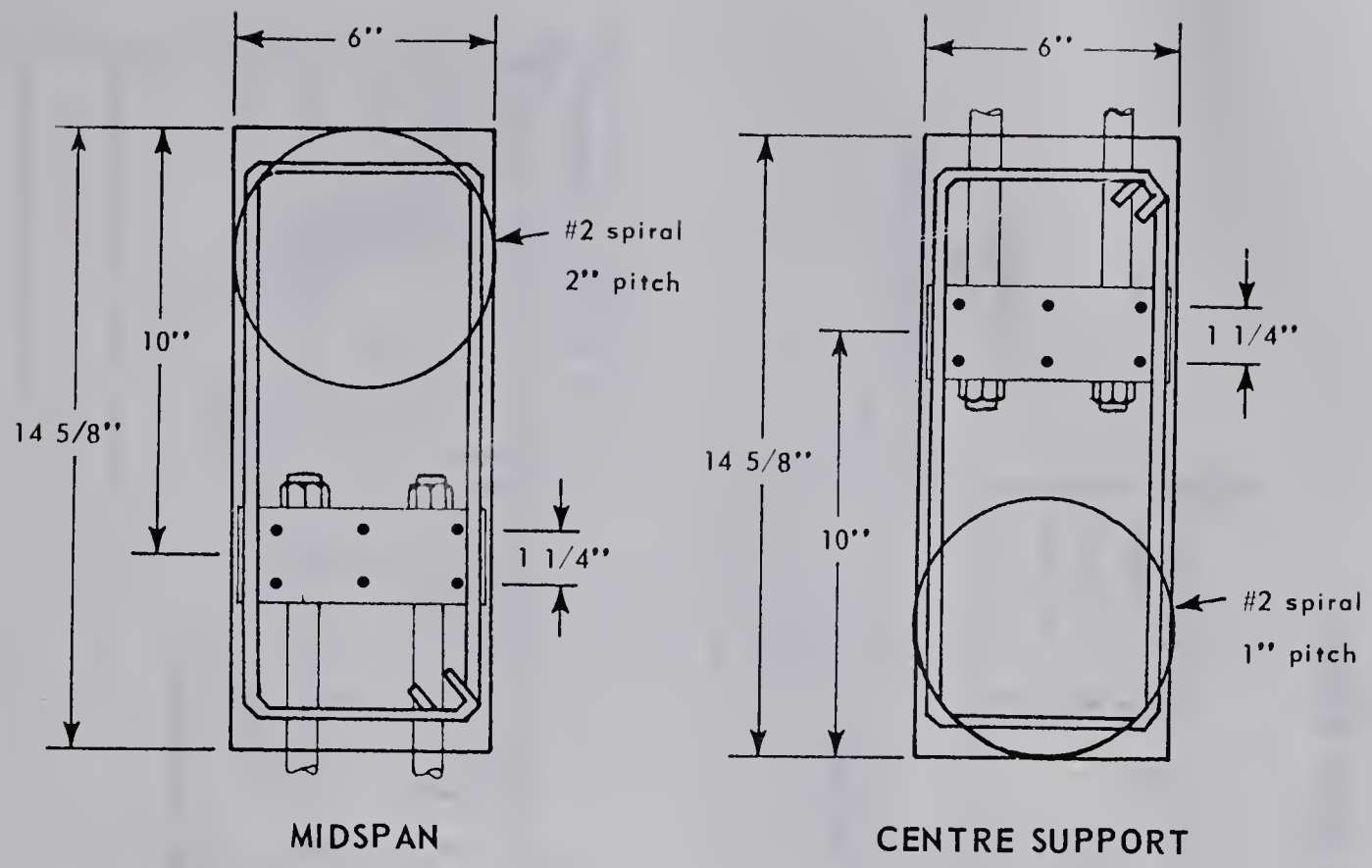

TYPICAL SECTION OF BEAMS WITH 6 STRANDS

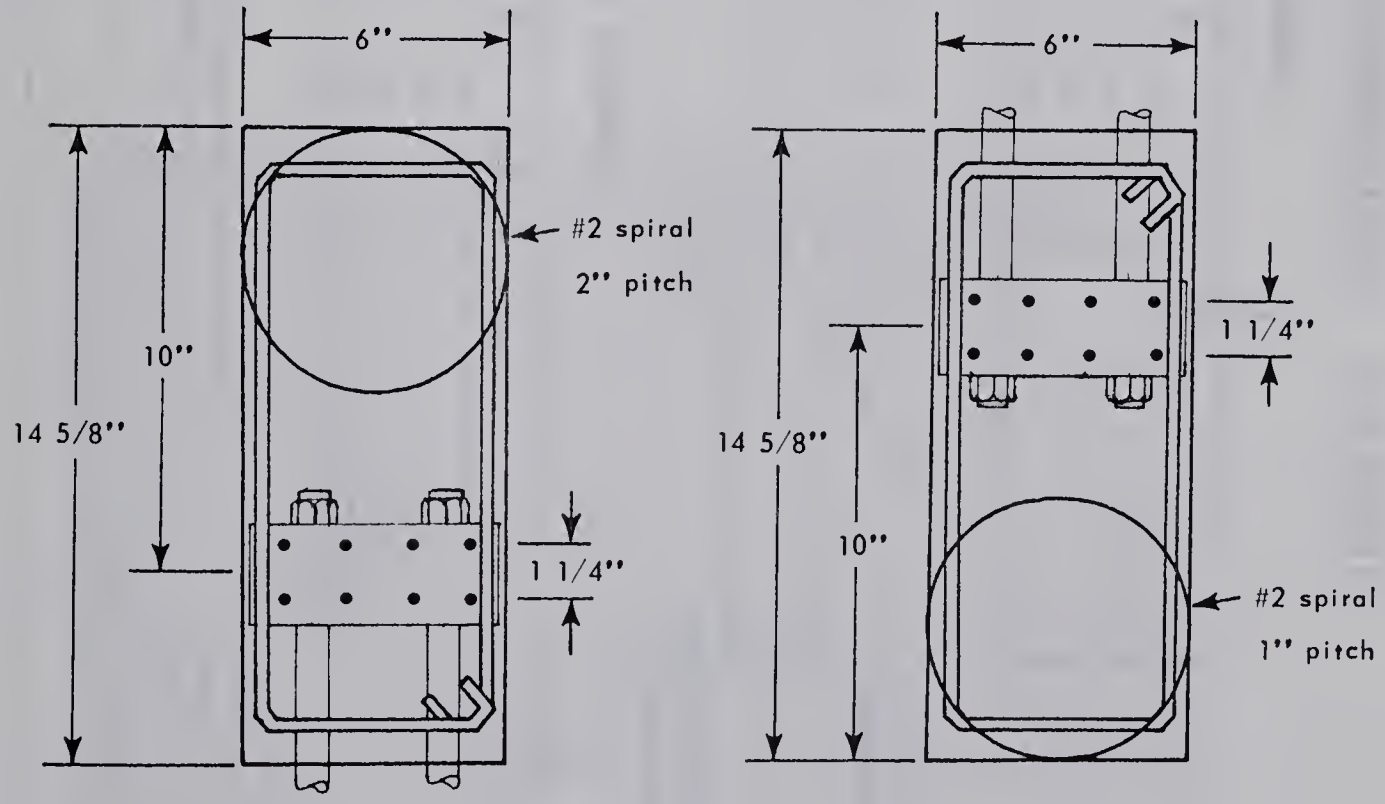

TYPICAL SECTIONS OF BEAMS WITH 8 STRANDS

FIGURE 3.3 TEST BEAM CROSS SECTIONS

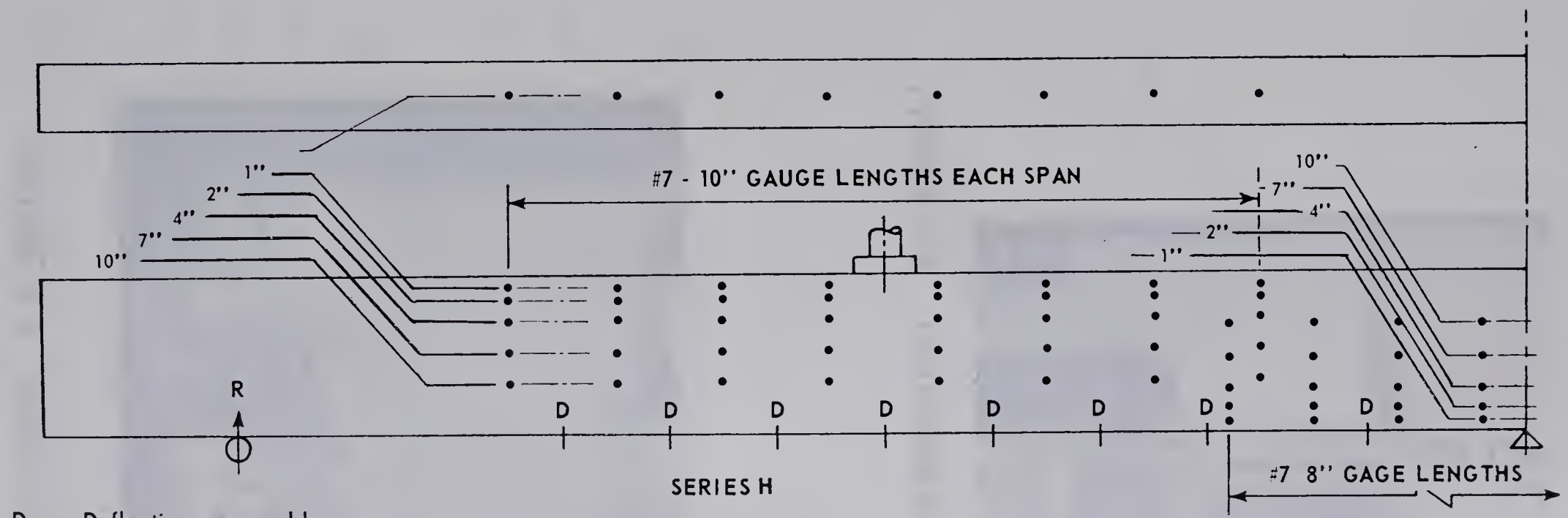

FIGURE 3.4 INSTRUMENTATION OF TEST BEAMS

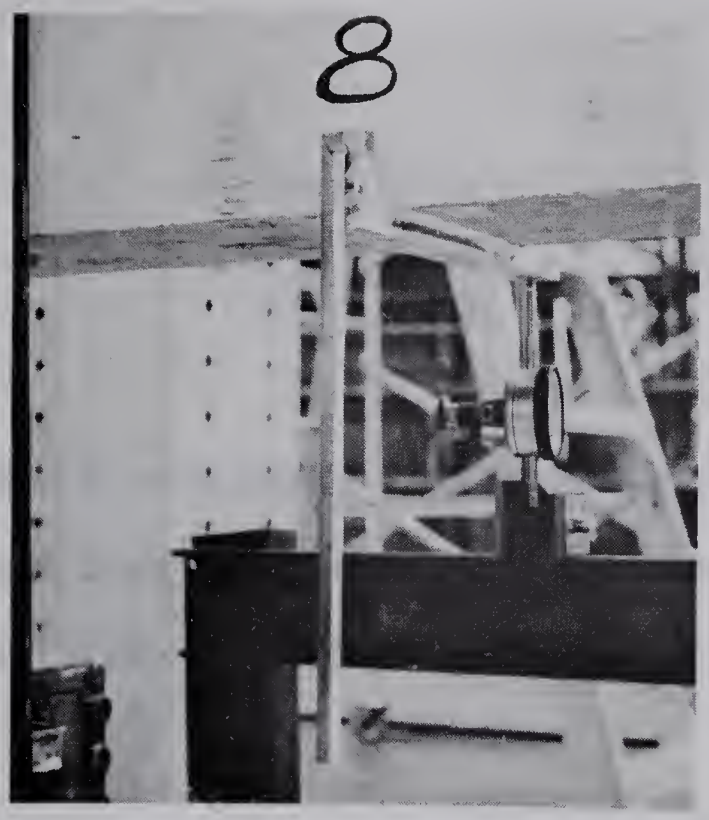

FIGURE 3.5 INSTRUMENTATION FOR DEFLECTIONS

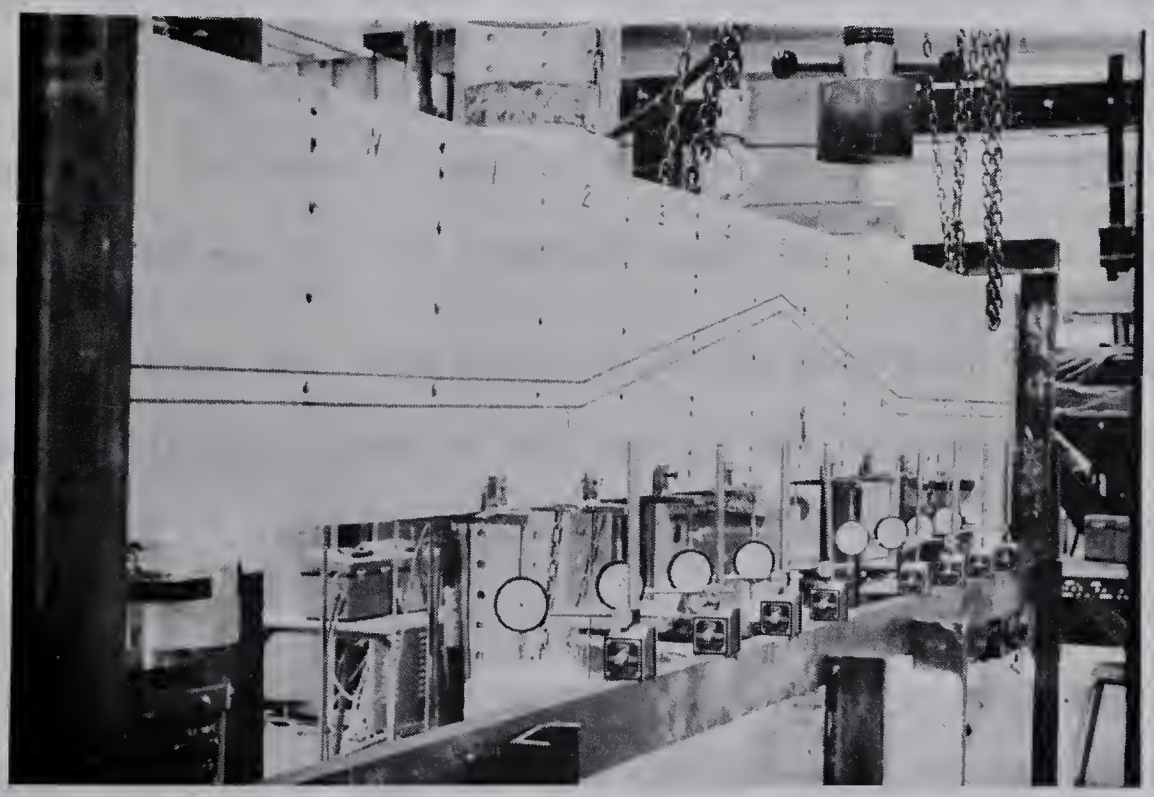

FIGURE 3.6 BEAM J.56 READY FOR TESTING

CHAPTER IV

TEST RESULTS

The direct measurements taken during each test were those of deflection and change in strain at every gage length, and exterior reactions. The locations of the instrumentation points are indicated in Figures 3.4 and 3.5.

The first two sets of results represent the variables which were measured directly. Figures 4.1 and 4.2 indicate the relationship between load and moment. The moment was calculated assuming point loads and reactions acting at their respective centre-lines. In both figures, the negative moment over the interior support is represented by the full line, and the positive span moment is represented by the broken line. The moments were calculated using the average of the two load-cell readings for the exterior reaction.

Deflections were measured at the centre of each gage length both by a dial-gage fixed to the base of the beam and by a survey-level reading on a graduated scale. The dial-gages, which gave readings to 0.001", were removed prior to the beam developing large deflections, after which the survey-level readings were used. Figure 4.3 shows the plot of applied load against measured deflection under each load point. During the final load increment in each test, the

only readings taken were those of deflection and reaction. An indication of the deformation occuring over this range is given on the load-deflection graphs by plotting the penultimate point, corresponding to the last increment at which strain-gage readings were taken.

The third and fourth groups of curves show the relationships which were derived from the measured readings. A complete set of strain readings was taken after each load increment. For each gage length, at each load increment, the distribution of strain was reduced to a "best fit" by the method of least squares. However, strains in excess of those corresponding to cracking were ignored in this analysis since a straight line distribution was affected by the opening-up of tension cracks. Curvature was defined as the slope of the strain distribution derived as above. Figures 4.4 and 4.5 show the moment-curvature relationships for all beams. Since strain readings were not taken after the penultimate load increment, these curves do not show the ultimate curvature. Reference to Figure 4.3 will indicate the amount of deflection occuring over the last increment, being a measure of the increase in curvature. An estimate of this ultimate curvature is made in Chapter 5. The ultimate moments achieved for each section are indicated by arrows.

Figures 4.6 and 4.7 show the distribution of derived curvature along the length of each beam. The calculated points, representing the curvature at the centre of each gage length, are connected by straight lines for simplicity. The distributions corresponding to three loads are shown.

Table 4.1 presents a summary of the test results, and indicates the loads at which the different modes of cracking were initiated. The letters 'N', 'C' and 'S' refer to the North, Central and South sections, respectively, of a beam and correspond to its orientation in the laboratory.

TABLE 4.1

A SUMMARY OF THE TEST RESULTS*

BEAM	TYPE OF FAILURE	Mcr.	Msp.	M_u	Psh. Cr.	Pu	Δmax.
H.108	Tension (N)	33.5 (C)	75.0 (C)	88.4 (N)	-	57.3	2.53 (N)
H.106	Tension (N)	21.5 (C)	76.2 (N)	80.0 (N)	36.0	48.0	1.73 (N)
H.106.C	Compression (S)	36.0 (C)	68.0 (S)	71.8 (S)	-	43.3	1.64 (S)
J.58	Tension (S)	34.5 (N)	92.5 (S)	105.0 (S)	84.0	124.0	1.20 (S)
J.56	Tension (N&S)	30.5 (C)	79.0 (N)	83.0 (N&S)	75.0	98.0	0.68 (N)
J.56.C	Tension (S)	26.5 (C)	73.5 (C)	81.3 (S)	75.0	99.0	0.90 (S)

* For details of the test beams see Table 3.1

N, C&S refer to the North, Centre and South sections respectively

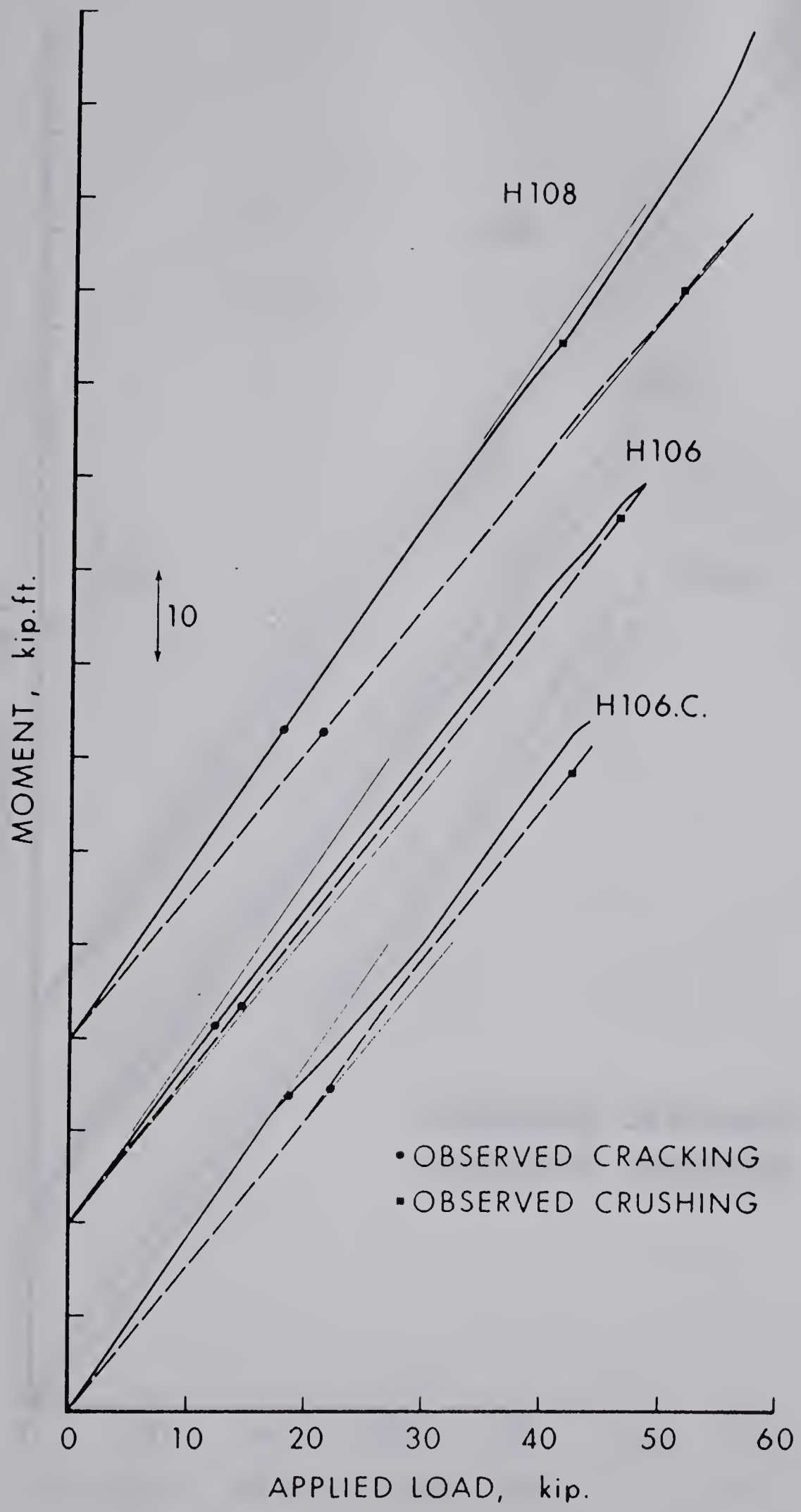

FIGURE 4.1 MOMENT-LOAD RELATIONSHIPS, SERIES "H".

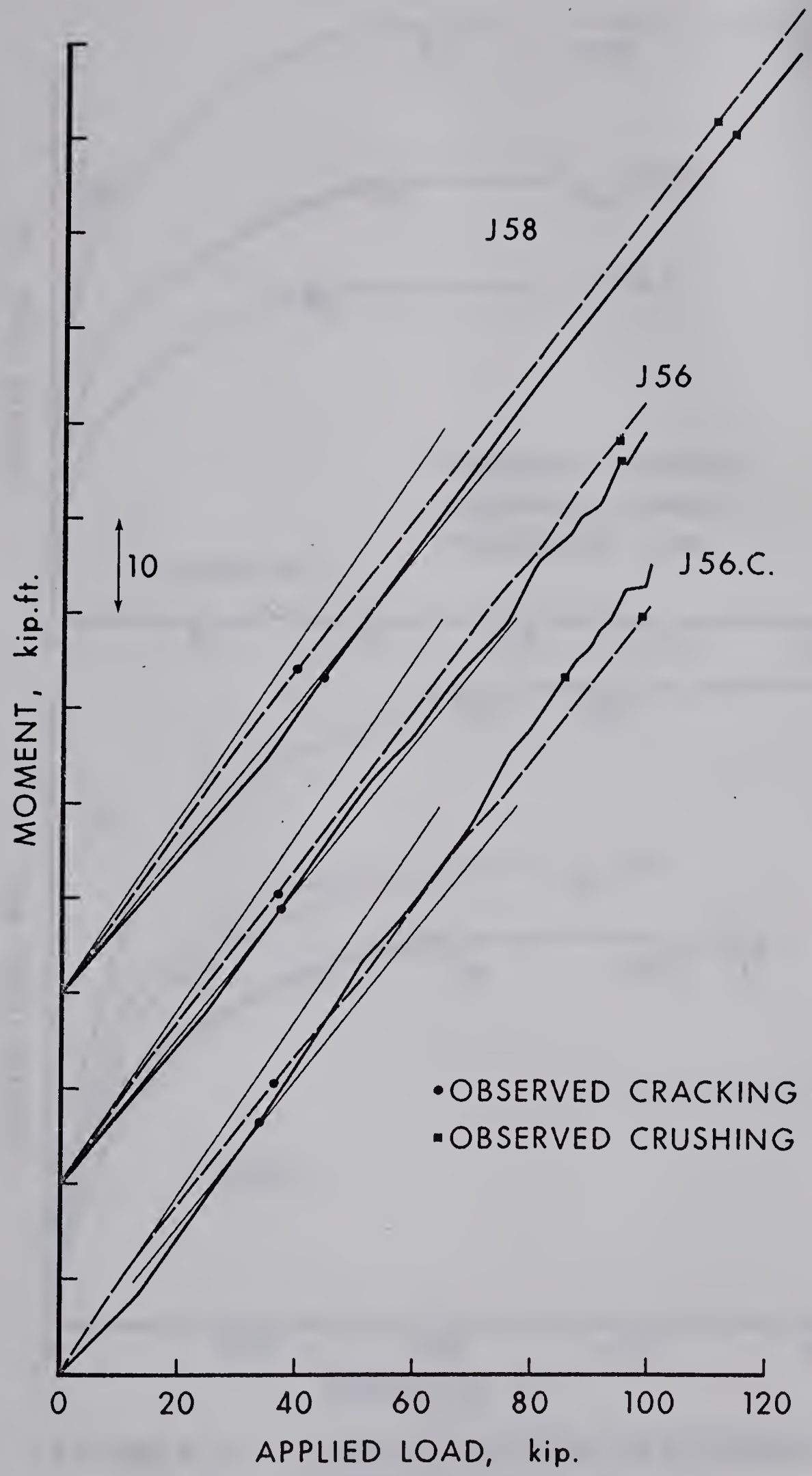

FIGURE 4.2 MOMENT-LOAD RELATIONSHIPS, SERIES "J".

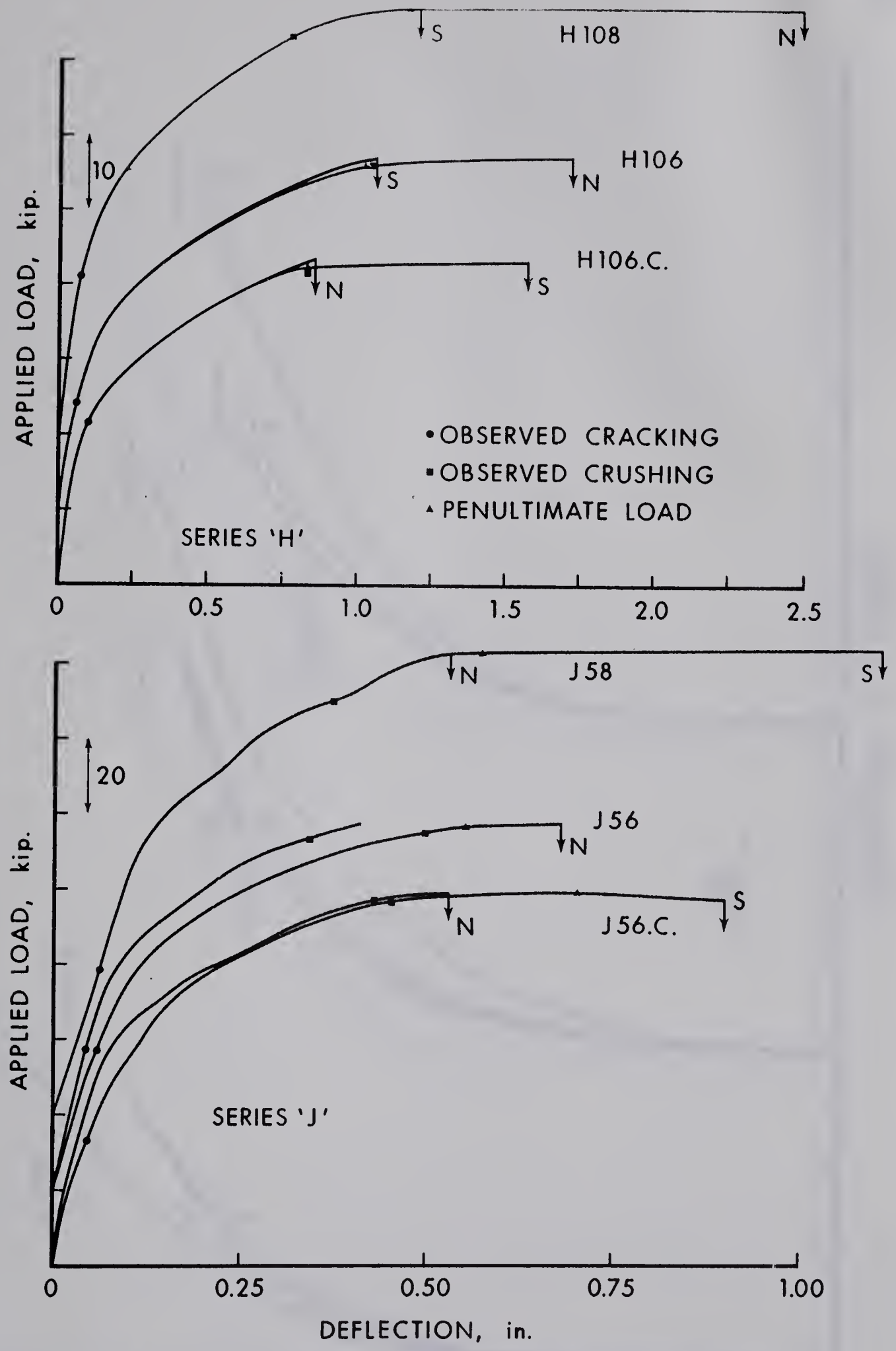

FIGURE 4.3 LOAD-DEFLECTION RELATIONSHIPS, SERIES "H" AND "J".

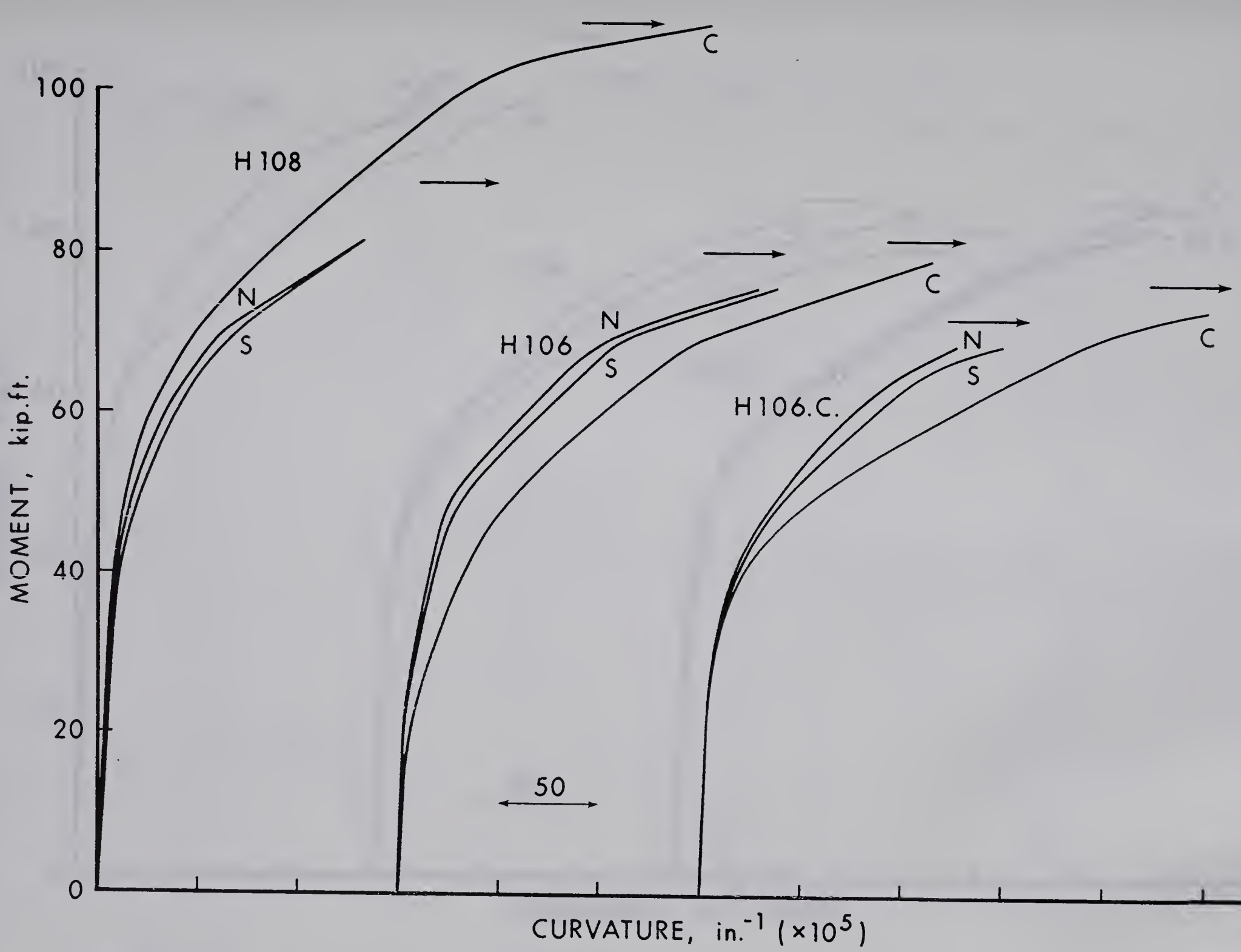

FIGURE 4.4 MOMENT CURVATURE RELATIONSHIPS, SERIES "H".

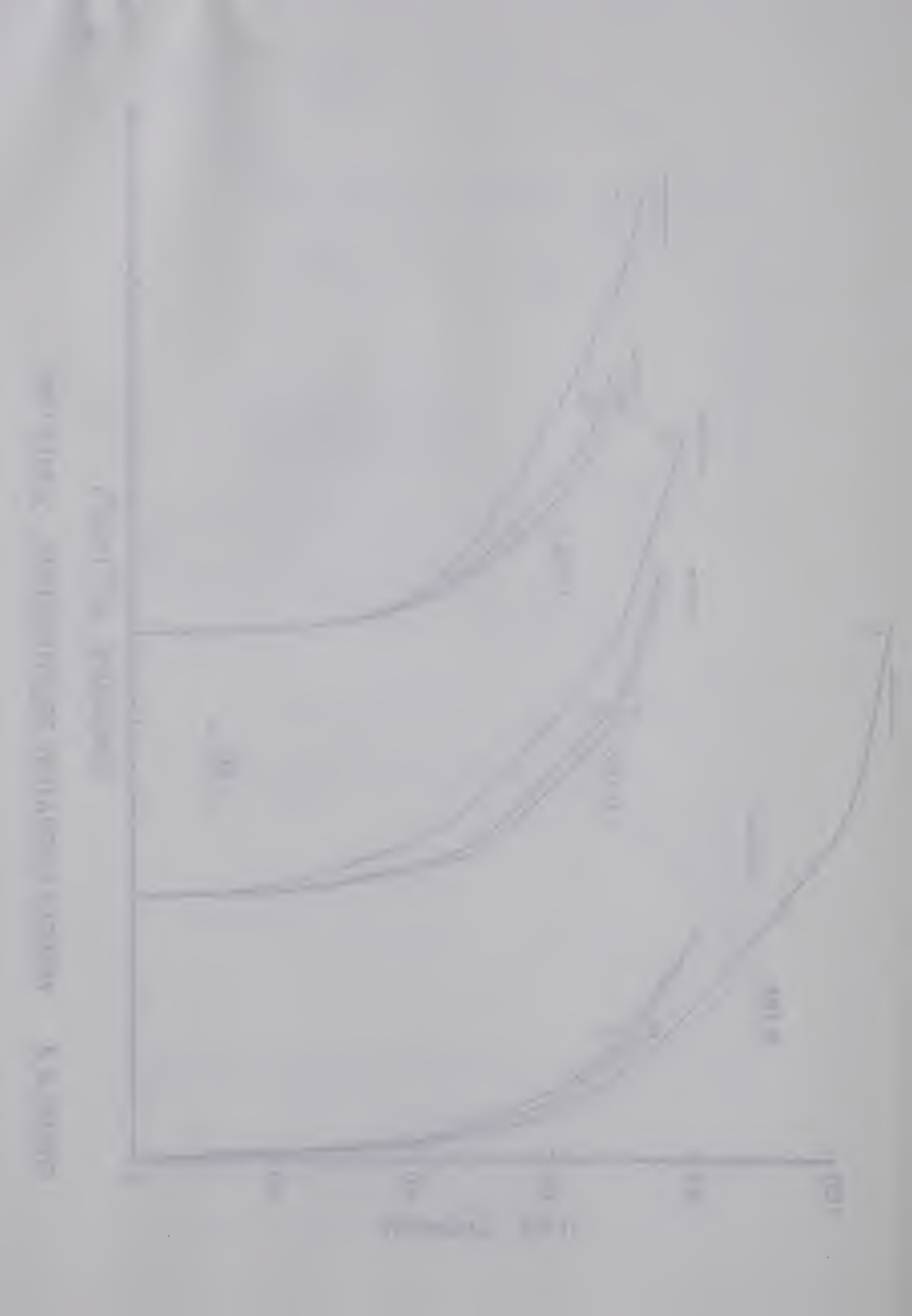

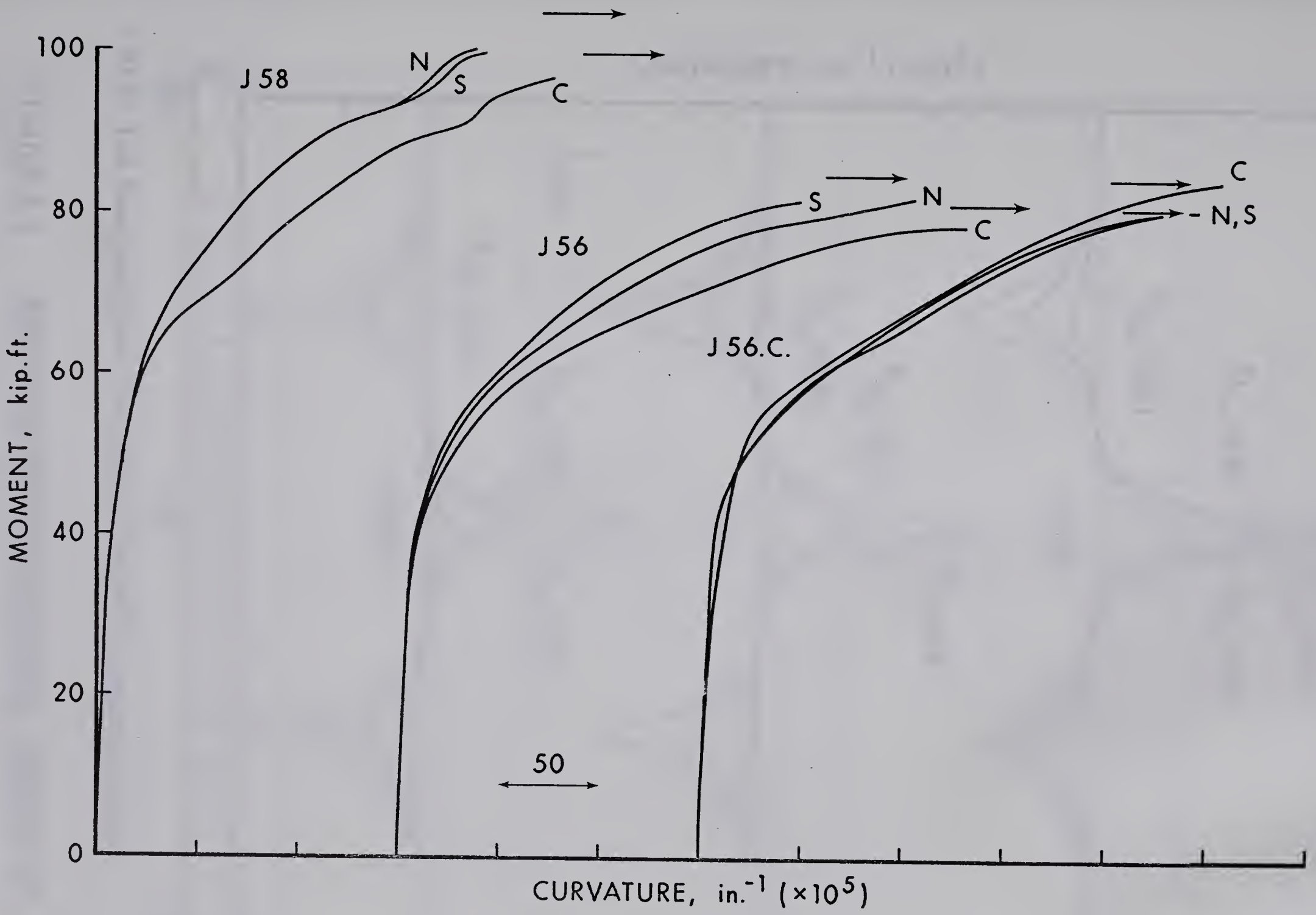

FIGURE 4.5 MOMENT CURVATURE RELATIONSHIPS, SERIES "J".

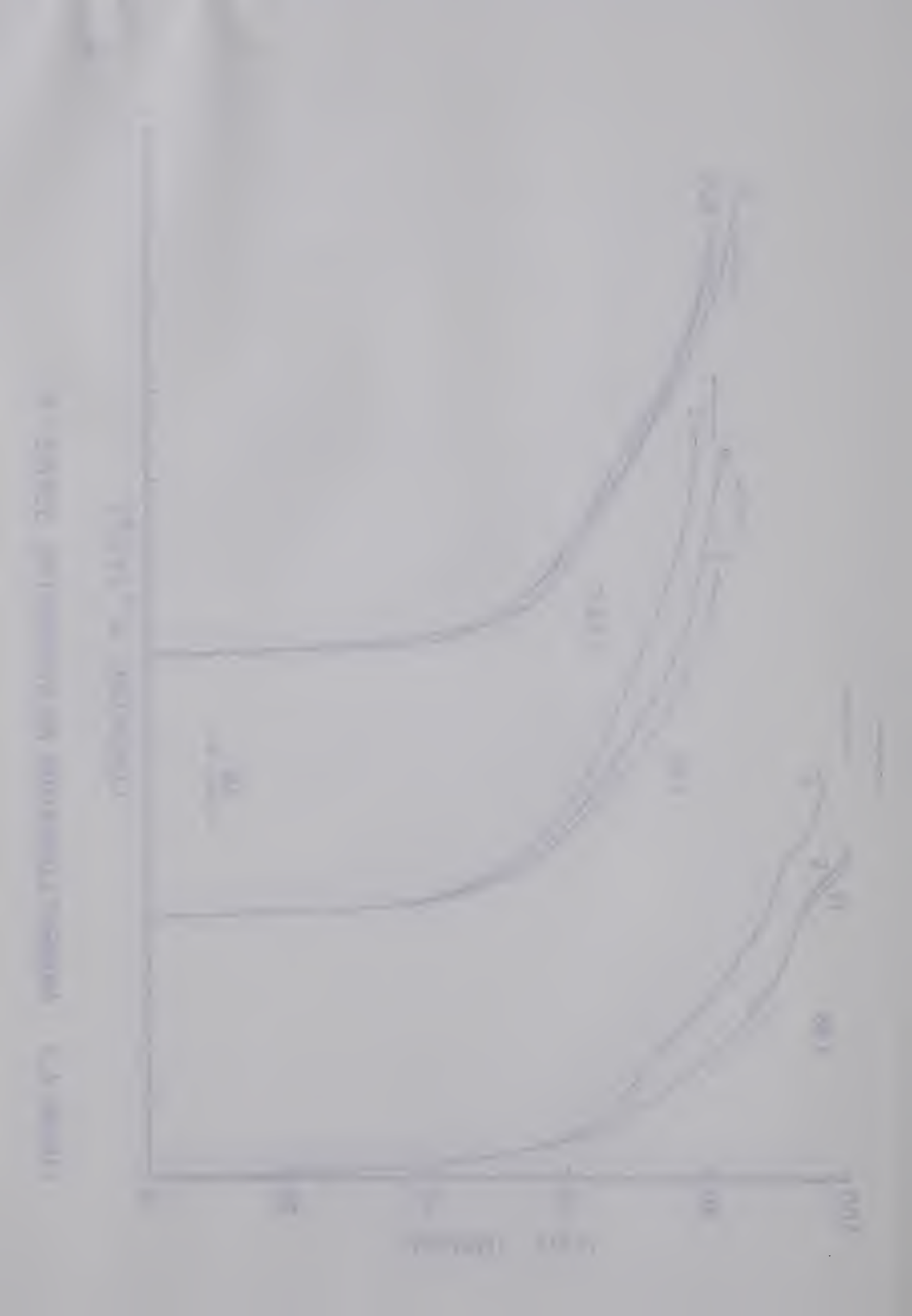

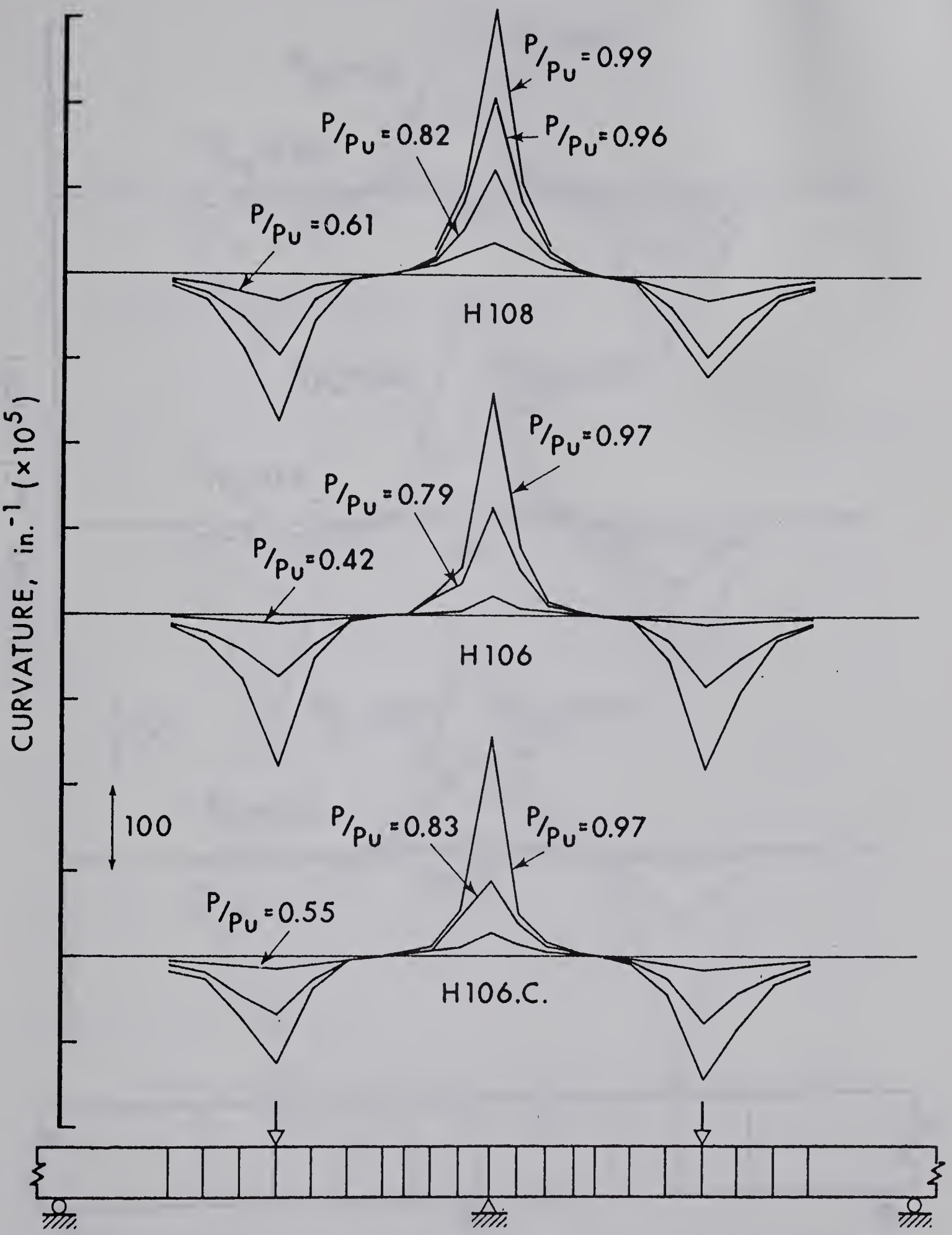

KEY: The lines represent the centre lines of the gage lengths.

FIGURE 4.6 DISTRIBUTION OF CURVATURE, SERIES "H".

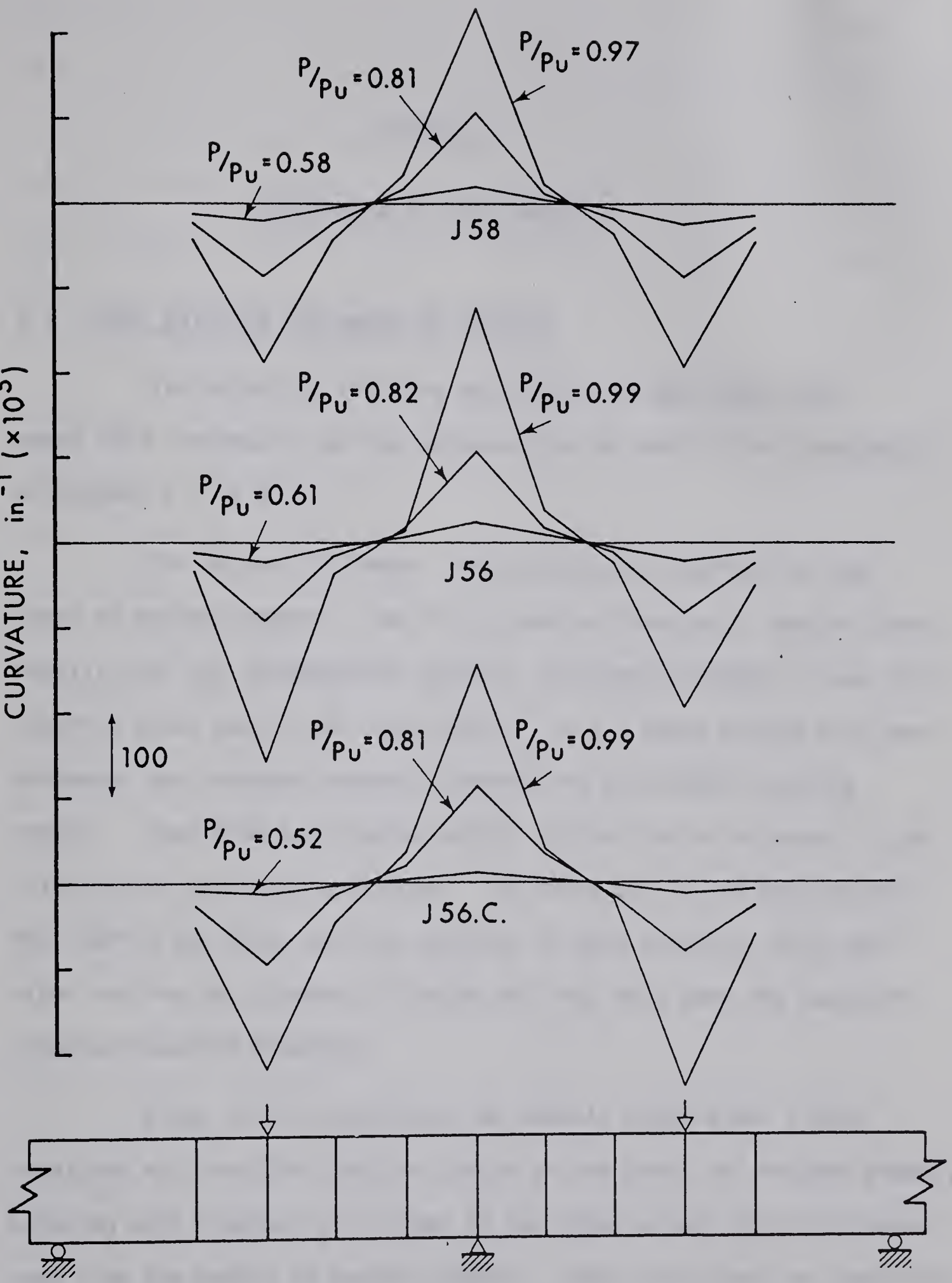

KEY: The lines represent the centre lines of the gage lengths.

FIGURE 4.7 DISTRIBUTION OF CURVATURE, SERIES "J".

CHAPTER V

DISCUSSION OF TEST RESULTS

5.1 Crack patterns and modes of failure

The extent of cracking was marked on each beam after every load increment, and the patterns can be seen in the photographs of Figures 5.1 to 5.4.

For Series 'H' beams, the cracking was confined to the zones of maximum moment. The first crack to form was a tension crack, usually over the intermediate support, although sometimes it was first observed under one of the load points. In all beams except one, good agreement was achieved between observed and calculated cracking moments. Beam H106 had cracked before testing due to an error in the releasing of prestress operation. The crack was in the compression zone during the test, and was observed to have closed up very soon after testing was started, although this may have been the cause of premature tension cracking.

After initial cracking, the overall pattern was slowly developed with vertical tension cracks at the points of maximum moment, becoming more diagonally inclined as the moment-shear ratio decreased away from the points of maximum moment. These cracks may be classified as "flexure-shear" cracks since the combined bending and shear stresses were critical in forming their diagonal branches. In those beams with spiral confinement, it was observed that the cracks did not intrude

above the level of the mid-depth of the spiral, while in the control beam, cracking was observed to extend to a correspondingly higher level.

Shear cracks were observed to form in beam H106 at a load of 36 kip. These cracks started at about mid-depth of the beam and were inclined at about 45 degrees. However, the extent of these diagonal tension cracks was not very great.

Crushing, and subsequent spalling, was observed in all Series 'H' beams. In all cases it occurred immediately adjacent to the bearing plates, indicating that a considerable amount of confinement, and hence additional strength, was being provided in the regions of the steel plates. This observation would appear to be similar to that made by Base and Read[2]. The presence of some confining effect due to a triaxial state of stress in these areas is quite evident. However, to what extent the rate of change in depth of the neutral axis has on the confining effect was by no means evident. It is suggested, however, that if this effect is significant in simply supported beams, as Base and Read propose, then its effect in continuous beams, where the moment gradient is usually steeper, might be more significant.

Failure was defined as the load after which the beam refused to accept a further increase in load. In most cases this was easily defineable by a tension failure, however the failure of beam H106.C was not so distinct. The tension failures of beams H108 and H106 were anticipated by a fairly ductile increase in deflection under one of the load points. Each of these two beams failed under the North load point. This appears to be further evidence of an unpredictable increase in moment capacity over the interior support,

where failure was expected. The primary failure resulted in the fracture of all of the prestressing strands. It is possible that the presence of the steel blocks and the holding-down bolts determined the position of the failure crack, however it is felt that this factor in no other way affected the results.

After the primary tension failure, a large crack was often developed a few feet away. This was probably caused by a cantilever effect and is of no significance.

Both tension failures in Series 'H' were accompanied by spalling, indicating that the failures would most probably have been in compression had there been no confinement.

The compression failure of beam H106.C indicated that the beam was over-reinforced. Reference to Table 3.1 will confirm that under the South load point, at which failure occurred, the ratio (p.fsu./f'c) is 0.349, which is in excess of the nominal value of 0.3. This was an unintentional result, being mainly due to a particularly under-strength batch of concrete.

The Series 'J' beams were considerably more distressed, at corresponding loads, than the same beams in Series 'H'. The first cracks to form were, as before, those starting at the tension face and becoming flexure-shear cracks at a later stage. At a load varying from 43% to 68% of the ultimate, diagonal tension cracks were observed to start at the mid-depth of the beams.

The modes of failure for the Series 'J' beams were similar to those for the Series 'H' beams except that the tension failures were not so ductile. All three beams failed in tension.

Beam J58 failed primarily under the South load point, by fracture of the strands accompanied by spalling. A secondary tension failure occurred over the interior support. Beam J56 failed by simultaneous rupture of the strands under the two load points, each accompanied by minor crushing. Beam J56.C failed in tension under the South load point at a slightly greater load than beam J56. This indicates that the presence of spiral confinement in no way increased the capacity of the nominally under-reinforced section.

The most outstanding observation from the failures of all six beams is the fact that no failure occurred over the interior support. It has been suggested[4] that the presence of confinement might tend to increase the moment capacity of an over-reinforced section. If it may be assumed that a closer pitch of spiral would result in a greater capacity in an over-reinforced section than in a similar section with a greater pitch, then this might have accounted for the failures of the #8 beams in each set, had they failed in compression. Again, in the case of a compression failure, the increase in ductility expected from a closer pitch of spiral might have diverted the failure to the span sections. However, in all cases, tension failures were produced, and so it can only be concluded from these observations that either a greater moment capacity or a greater deformation capacity was achieved at the interior support, thus attracting failures to the spans.

In an attempt to reduce the confining effect over the interior support, a smaller bearing plate was used for Series 'J' beams than for Series 'H'. However, this had no visible effect on the failure.

An effect of the shear cracks in Series 'J' beams was to disrupt the linearity of the strain distribution to the extent that the tension strains measured over the gage lengths would often be greater at the 7" depth than at the 10" depth. Hawkins[5] defined this situation as a shear failure. However, in the absence of any shear cracks which might have attributed to the failure of any one of the beams, all the failure modes have been described as flexural.

Due to the load maintainer in the system, it was impossible to prevent the severe deformations occurring after the ultimate load had been reached. Figures 5.1 to 5.4 indicate the state of the beams after collapse, and hence, not necessarily at the ultimate load.

5.2 Moment-load relationships

The elastic moment distribution in the test beams, assuming them to have uniform stiffness and to be supported and loaded at points, was such that the maximum positive moment (5/32.P.L.), caused by the two applied loads P , was five-sixths of the negative moment (6/32.PL.). These distributions are indicated on the graphs by the thinner lines emanating from the origin; the upper one corresponding to the negative moment over the interior support, and the lower one to the positive span moment. The measured moment-load relationship for the interior support is represented by the full line, and that for the span sections by the broken line.

The moment-load relationships for Series 'H' beams, (Figure 4.1), indicate varying degrees of moment redistribution. Beam H108 displayed no redistribution until crushing occurred at the interior

support, when a slight shift from the elastic distribution may be observed. At the ultimate load the two paths tended to diverge.

Beam H1O6 developed full redistribution at the ultimate load, though there is no evidence of ductile behaviour prior to failure. An ideal moment-load relationship would show the two paths converging at a moment less than ultimate and continuing to increase simultaneously. Beam H1O6 indicated convergence from the beginning of loading. It is possible that the crack which was developed before testing might have provided some small amount of rotational freedom at the interior support, thus resulting in a premature departure from the theoretical elastic distribution.

Beam H1O6C, displayed some amount of redistribution, commencing at the cracking moment. However, full redistribution was not achieved.

The moment-load curves for Series 'J' beams display no resemblance to the corresponding curves for Series 'H'. All the 'J' beams behaved in a manner which was inconsistent with either elastic or plastic distribution of moments. Since, for all three beams, the positive span moments were greater than the negative support moments over the greater part of the range, then there is little meaning to redistribution of moments in the usual sense.

This behaviour could be explained, to an extent, if the interior support had not been in contact with the beam, thus producing a larger reaction at the outer support than would be normal for full continuity. However, as soon as proper contact was achieved, the slope of the distributions should have reverted to the theoret-

ical. In fact, this phenomenon can be seen to have happened in all three series 'J' beams. At loads varying from 12 kips for J56.C to 36 kips for J58 there is quite a distinct change in slope of the distributions indicating that this might be the reason. However, it was felt, that by providing a seating of Plaster of Paris between the beam and each of its supports such a situation should not arise and that a firm support would be provided. It is difficult to explain this behaviour in any other way.

It is of interest to note that Hawkins obtained similar behaviour with some of his beams. Although 21 out of 24 of his beams had I sections, it is suggested that the trend of the moment-load plot would be the same.

5.3 Load-deflection relationships

The measured load-deflection relationships are presented in Figure 4.3. These curves represent that full range of ductility achieved in the tests, whilst values of curvature are limited in range to those values reduced from the penultimate load readings of strain. In order to illustrate the increase in deformation which occurred during the ultimate load increment, the appropriate points are plotted on these curves.

The outstanding feature of the load-deflection curves is the greater ductility attained by the #8 beams in each set, whilst little difference is noticed between the #6 and the #6.C. This would imply that little has been achieved, in the way of increased ductility, by including spiral confinement in the nominally under-reinforced sections.

In general, a good degree of symmetry was obtained between the deflections of the North and South spans. However, in beams J56 and J56.C, a small initial discrepancy is quite evident. This behaviour is reflected in the distribution of curvature plot shown in Figure 4.7. It is possible that this initial difference in deflection determined the final location of failure. This may again be accounted for by a fractional difference in support heights, although particular care was taken to observe any initial settlements; none was observed.

It was usually possible to predict when failure was imminent. The survey level was focused onto the appropriate scale and the readings were carefully watched. At the instant of failure, the reading was recorded as the ultimate deflection, although further deformation usually occurred as a result of the strain energy in the loading system.

5.4 Moment curvature relationships

Figures 4.4 and 4.5 show the derived moment-curvature relationships. Moment was defined as the product of measured load and lever-arm equal to the distance between centres of appropriate loads. Curvature was defined as the slope of the "best-fit" straight line distribution of strain readings. It was not possible to present the full range of curvature, since measurements of strain were not taken for the final load increment. However, the ultimate moments are indicated for each section by an arrow.

In general, the discrepancies between the curves for the North (N) and South (S) sections are within acceptable tolerances.

However, the differences between the interior support (C) and the span section curves imply an inherent difference in the characteristics of the two sections. This may be a result of the difference in the strand profiles at the two sections. The effect of confinement due to the bearing plate may also influence the behaviour. There is no consistency in the position of the interior support curve with respect to the span curve. However, in all beams, except H108, the negative moment curve lies beneath the positive moment curve.

The plot for beam H108 warrants further discussion. The failure section (see Table 4.1) was the North span, corresponding to an ultimate moment of 88.4 kip. ft. and a curvature well in excess of 140×10^{-5} in.$^{-1}$. At the same load, the moment at the interior section was calculated to be 108.5 kip.ft. and a curvature in excess of 306×10^{-5}. Again, it is difficult to explain this behaviour, but it would seem that considerable amounts of reserve strength were being developed due, probably, to the confining effect of the triaxial state of stress which undoubtedly existed above the bearing plate. The curvature developed at the interior section is not excessive.

In view of the large moments being developed, it is of significance to compare the corresponding moments at the edges of the bearing plates, at which positions it is unlikely that there can be any external influence. Table 5.1 presents this comparison. It can be seen from Table 5.1 that for the Series 'J' beams, where the moment gradient is particularly high at failure, a considerable difference in moments is calculated, whereas for Series 'H', the difference is significant but not so great. Since all crushing of the concrete

occurred adjacent to the bearing plates, it is suggested that these revised values of moment are a more realistic estimate of the internal forces in the beams.

5.5 Distribution of curvature

Figures 4.6 and 4.7 represent the magnitude and distribution of derived curvature. These plots, at different stages of loading, indicate the manner in which the distribution of curvature changes. At loads up to about 50% of the ultimate, the distribution is still almost linear, with slight peaks at points of maximum moment; these peaks then becoming more pronounced, and confined to the zones near to the points of maximum moment.

The distribution of curvature provides an indication of the distribution of deflection, and vice-versa. At failure, the magnitude of curvature indirectly reflects the magnitude of the compressive strains, for those beams failing in tension. An indication of the strains achieved at the penultimate load are presented in Table 5.2.

5.6 Estimation of ultimate curvatures. Rotations

Curvature and rotation, in reinforced concrete beams, are almost synonymous, and for this reason the two are dealt with together. The internal rotation occurring in a length of beam is defined as the integral of the curvature with respect to the length. In this series of tests, curvatures were derived from the strain readings over a 10" (or 8") gage length and therefore they are essentially only average values, since there is always a moment gradient across each gage length. Since most inelastic rotation occurs within one of these gage lengths, then to plot moment against rotation would be simply to reproduce the moment-curvature graph with a different scale on the deformation axis. In fact, there was found to be a spread of inelastic rotation away from the points of maximum moment, but a moment-rotation plot would still be similar to a moment-curvature plot, and for this reason such a set of curves was not presented.

However, it is of interest to discuss the rotations in the beams. Rotations were calculated by summing the area beneath the distribution of curvature plots (Figures 4.6 and 4.7) at different loads.

Mattock[6] and Corley[7] have each approached the problem of rotations in generally the same way. Each has proposed an expression for the plastic rotation occurring over an arbitrary length of beam in terms of the section properties, and then modified this to include the spread of plasticity along the length of the beam. The modification factor is a function of the parameter Z/d, which is itself a function of the geometry of the beam and the loading conditions.

In order to illustrate both the magnitude and distribution of rotation along the beams, Table 5.3 presents the amount of rotation occurring, at the penultimate load, in an arbitrary length of d/2 each side of the points of maximum moment. Also tabulated is the ratio of the rotation in d/2 as a function of the total rotation occurring in each shear span, Z . The three shear span zones are indicated in the key drawing below Table 5.3. The ratios, r_1 etc., were used in the calculations for the estimation of ultimate curvatures, which are outlined, with an example, in Appendix C.

Over the length of beam in which the strand profile is horizontal, Zone 1, it is evident from Table 5.3 that the ratio, r , is a function of the moment gradient, which might be expected. Between 33% and 55% of the total rotation in the Zones 1 occurred over a length of 5", equal to d/2 . However, over the length of beam with the sloping profile there is no such tendency. In these two zones the ratio was between 58% and 81%.

It is of significance to have at least an estimate of the values of ultimate curvature. A method was devised for estimating these values from the measured values of ultimate deflection. The results of the method were found to compare favourably with those calculated from the distribution of strain. Even acknowledging a degree of approximation, it may be seen from Table 5.4 that the #8 beams in each series indicate a much higher ultimate curvature than the #6 and #6.C, whilst nothing apparently was gained by including confinement in the #6 beams. The values of ultimate curvature may be compared with those theoretically derived in Appendix B.

5.7 Comparison of results with previous tests

Both Ward[3] and Wilkinson[4] used the same nominal cross-sections in their series as were used in the present test series. Table 5.5 presents a summary of Ward's results, and Table 5.6 presents a summary of Wilkinson's results. For the present series, the section properties are presented in Table 3.1 and the test results in Table 4.1.

Tables 3.1, 5.5 and 5.6 include the parameter $\frac{p.f_{su}}{f'_c}$. This was chosen as a means of comparison because it can be related to the ACI Code requirements. However, the term f_{su} has not been used in its strict meaning, which is the steel stress at failure. Instead, the ultimate strength, f'_s , has been substituted for f_{su} in all the tabulated values, and is therefore a common factor in all of them. It is suggested that, for the beams reported here which failed in tension, f'_s is a good approximation to f_{su} , though for the beams failing by other than rupture of the steel the difference between f'_s and f_{su} may be up to 10%. The parameter $\frac{p.f_{su}}{f'_c}$ is therefore, at best, only an indication of the reinforcement index.

Ward tested his beams under constant moment. He assumed that curvature was also constant in this zone. It is suggested, therefore, that his results should not be influenced by the external effects which were encountered in this present series, and that his values of M_u and ψ_u should be the closest to the theoretically derived values, which are presented in TAble B1.

Wilkinson introduced a moment gradient, thus more closely representing the loading in a structural member. Although the be-

haviour of his beams was influenced by shear, all but one with a 1" spiral pitch failed in tension.

Both Ward and Wilkinson used slightly lower concrete strengths than were adopted for this series. As a result, the comparative beams with the lower reinforcement ratio are not necessarily under-reinforced in terms of the ratio $\frac{p.f}{f'_c}_{su}$.

However, some general comparisons are valid:-

(a) For beams with similar sections (H108, F2, and C2 and C4), those tested under constant moment reached the lowest ultimate moments and curvatures, whilst little difference is noticed between the ultimate moments of Wilkinson's beams and those in the present series. (It should be noted that, for the present series, the ultimate moments referred to are those occurring at the failure section and not necessarily the maximum moments in the beam at failure).

(b) All beams in the present series failed in the spans, where the spiral pitch was 2". A comparison of those sections with a 2" pitch indicates slightly higher moments in the present series. This observation might be relevant for those beams failing in tension, however for those failing in compression or shear-compression, it is probably due to differences in the concrete strengths.

A useful comparison, which is beyond the scope of this report, would involve the distribution of inelastic rotations, since this is likely to be a function of moment gradient and would probably be affected by continuity.

TABLE 5.1

MODIFICATION TO BENDING MOMENTS

BEAM	Measured reaction at ultimate load (R_u kip.)	Ultimate load (P_u kip.)	Span moments (kip. ft.)		Support moments (kip. ft.)	
			$M_{(1)}$	$M_{(2)}$	$M_{(1)}$	$M_{(2)}$
H108.	17.65	57.3	88.4	83.7	108.5	100.0
H106.	16.0	48.0	80.0	76.0	80.0	72.0
H106.C	14.4	43.3	71.8	68.4	73.0	66.0
J58	42.0	124.0	105.0	98.0	100.0	86.0
J56	33.2	98.0	83.0	77.5	79.0	68.0
J56.C	32.5	99.0	81.3	75.7	86.0	73.0

N.B. (1) Refers to the moments calculated assuming centre to centre dimensions

(2) ....." "....." "....." ".... edge of bearing block dimensions

TABLE 5.2

A SUMMARY OF DERIVED MAXIMUM STRAINS*

		SOUTH			CENTRE			NORTH		
BEAM	P/P_u	Comp. Strain	Tension Strain	Curv. x 10^5 (in^{-1})	Comp. Strain	Tension Strain	Curv. x 10^5 (in^{-1})	Comp. Strain	Tension Strain	Curv. x 10^5 (in^{-1})
H108	0.96	0.00356	0.0125	116	0.00894	0.0260	306	0.00496	0.0164	169
H106	0.97	0.00550	0.0173	184	0.00700	0.0236	264	0.00526	0.0169	178
H106.C	0.97	0.00398	0.0151	148	0.00544	0.0239	251	0.00315	0.0137	125
J58	0.97	0.00585	0.0186	194	0.00554	0.0181	188	0.00484	0.0229	227
J56	0.99	0.00451	0.0208	198	0.00561	0.0275	279	0.00483	0.0262	255
J56.C	0.99	0.00514	0.0244	243	0.00554	0.0249	255	0.00520	0.0221	221

* All values refer to the penultimate load

TABLE 5.3

A COMPARISON OF ROTATIONS

		ZONE 1			ZONE 2			ZONE 3		
BEAM	P/P_u	$\Theta_{(d/2)}$ rad.	r_1	Moment gradient kips.	$\Theta_{(d/2)}$ rad.	r_2	Moment gradient kips.	$\Theta_{(d/2)}$ rad.	r_3	Moment gradient kips.
H108	0.96	0.0085	0.37	17.2	0.0058	0.58	37.8	0.0103	0.58	37.8
H106	0.97	0.0089	0.39	15.2	0.0092	0.60	30.8	0.0132	0.74	30.8
H106.C	0.97	0.0063	0.33	13.7	0.0074	0.61	28.3	0.0125	0.81	28.3
J58	0.97	0.0079	0.48	40.2	0.0076	0.62	77.4	0.0089	0.68	77.4
J56	0.99	0.0100	0.55	33.0	0.0099	0.66	63.0	0.0110	0.71	63.0
J56.C	0.99	0.0098	0.48	32.2	0.0093	0.69	67.0	0.0100	0.59	67.0

Note: $r = \Theta_{(d/2)} / \Theta_{(z)}$

Key:

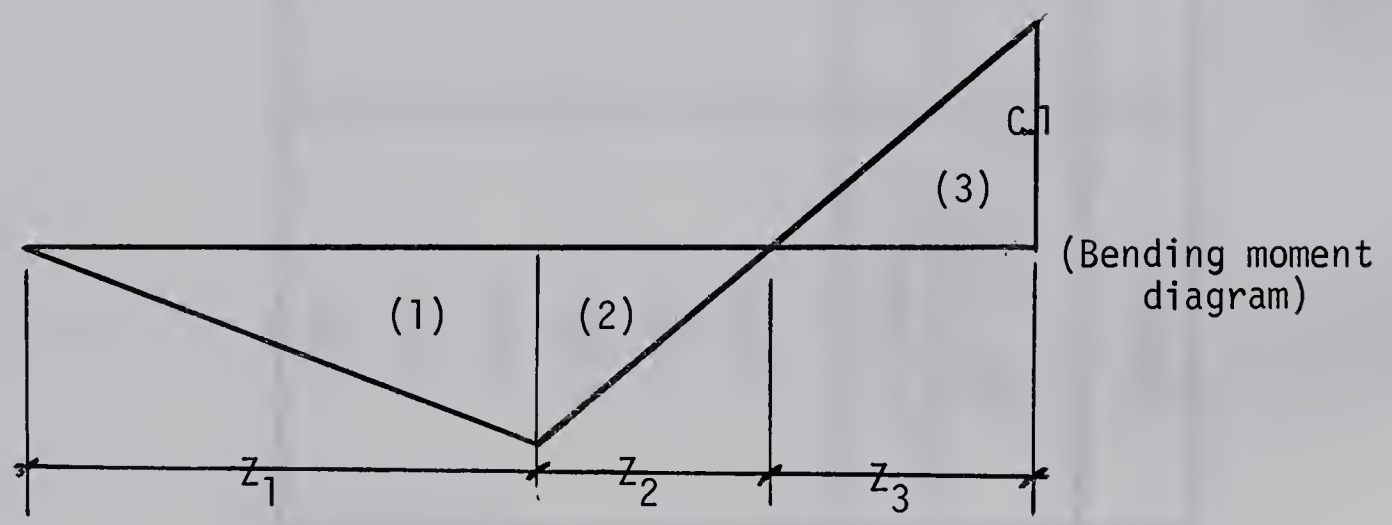

TABLE 5.4

ESTIMATE OF ULTIMATE CURVATURES*

BEAM	PENULTIMATE		ULTIMATE
	ψ (x 10^5) (From Strain Readings)	ψ (x 10^5) (From Deflection Readings)	ψ_u (x 10^5) (From Deflection Readings)
H108	169 (N)	200	628
H106	178 (N)	181	401
H106.C	148 (S)	142	480
J58	194 (S)	209	609
J56	255 (N,S)	227	314
J56.C	243 (S)	285	405

* For the calculations, see Appendix C

TABLE 5.5

A SUMMARY OF THE RESULTS OF WARD'S SERIES[3]

BEAM	SPIRAL		A_s sq.in.	$\frac{p.f_{su}}{f'_c}$	EFFECTIVE PRESTRESS (ksi)	MODE OF FAILURE	M_u (k.ft.)	ψ_u
	DIAMETER	PITCH						
A1	#1-6"	1"	0.46	0.41	147	BOND	-	290
A2	#1-6"	1"	0.35	0.30	140.4	TENSION	63.3	310
A3	#1-6"	1"	0.35	0.47	130.9	TENSION	59.4	430
A4	#1-6"	1"	0.46	0.61	128.5	BOND	70.2	330
B1	#2-3"	1"	0.46	0.37	137.7	BOND	79.8	210
B2	#2-4"	1"	0.35	0.32	141.7	TENSION	69.4	270
B3	#2-4"	1"	0.35	0.50	132.6	TENSION	63.9	430
B4	#2-4"	1"	0.46	0.65	130.2	BOND	77.8	430
C1	#1-6"	3"	0.46	0.42	138.7	COMP.	75.7	115
C2	#1-6"	2"	0.46	0.42	140.3	COMP.	76.2	180
C3	#1-6"	3"	0.46	0.57	127.6	COMP.	67.2	165
C4	#1-6"	2"	0.46	0.56	130.3	COMP.	72.3	175

Note: All beams tested with zero moment gradient

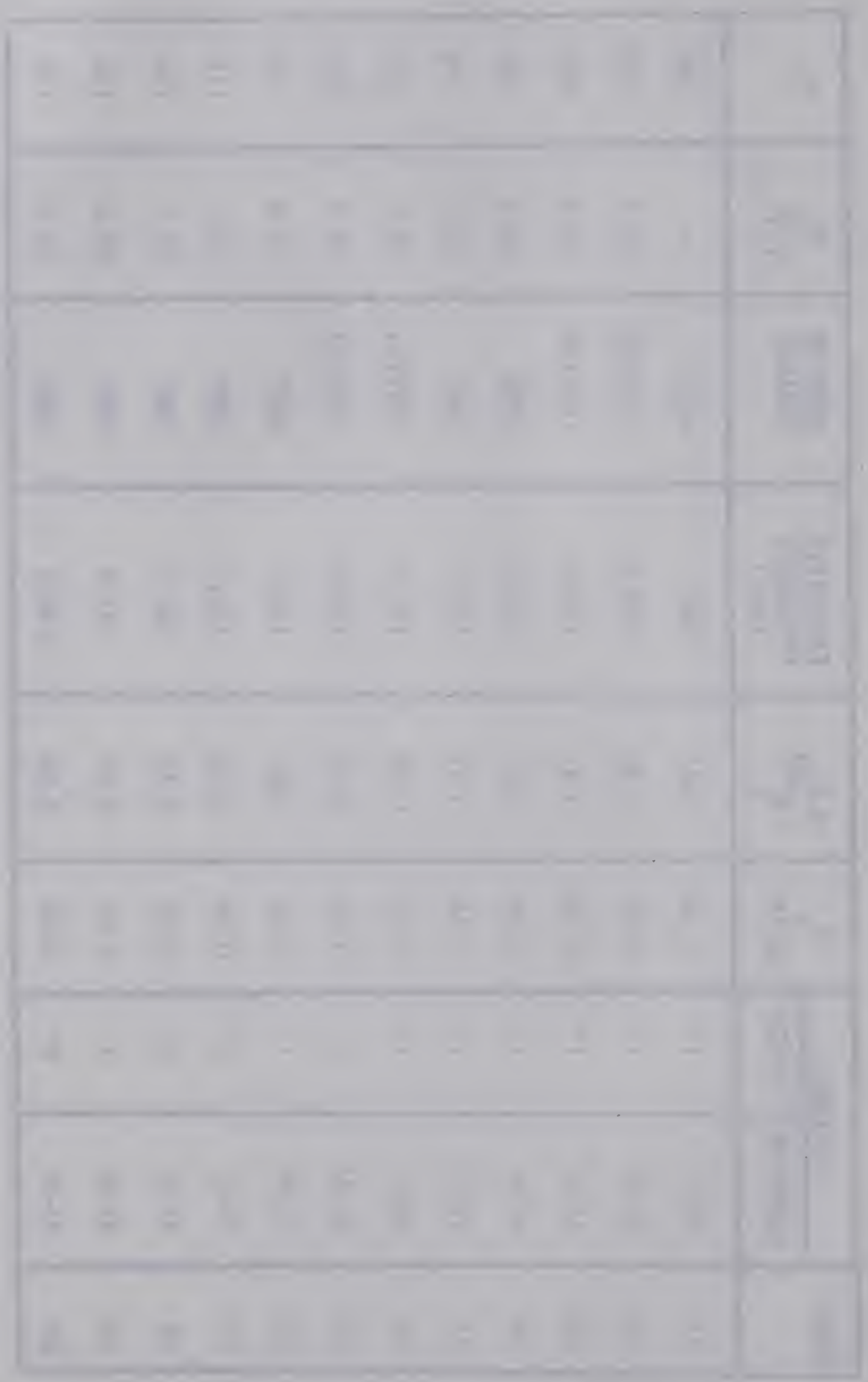

TABLE 5.6

A SUMMARY OF THE RESULTS OF WILKINSON'S SERIES[4]

BEAM	SPAN	SPIRAL PITCH	A_s (sq.in.)	$\frac{p.f_{su}}{f'_c}$	EFFECTIVE PRESTRESS (ksi)	MODE OF FAILURE	MOMENT GRADIENT (kip)	M_u (k.ft.)	ψ_u
D1	10'	1"	0.35	0.46	131	TENSION	14.2	71.2	370
D2	10'	2"	"	0.41	135	COMP.	13.7	68.2	408
D3	10'	3"	"	0.41	135	COMP.	13.2	66.2	254
E1	5'	1"	"	0.43	132	SHEAR	28.8	72.2	350
E2	5'	2"	"	0.37	138	TENSION	30.5	76.3	234
E3	5'	3"	"	0.45	134	COMP.	28.5	71.2	274
F1	10'	1"	0.46	0.40	144	TENSION	18.7	93.5	320
F2	10'	2"	"	0.42	129	TENSION	18.8	94.0	356
F3	10'	3"	"	0.60	127	SHEAR/COMP.	14.4	72.0	246
G1	5'	1"	"	0.40	149	TENSION	43.2	108.2	424
G2	5'	2"	"	0.45	132	SHEAR/COMP.	37.2	93.1	327
G3	5'	3"	"	0.58	135	SHEAR/COMP.	33.5	83.7	244

Note: Spiral diameter = 6" in all beams

NORTH

SOUTH

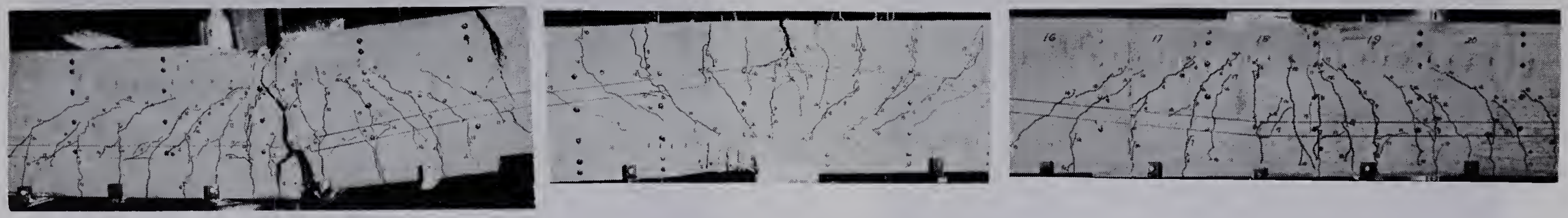

H.108

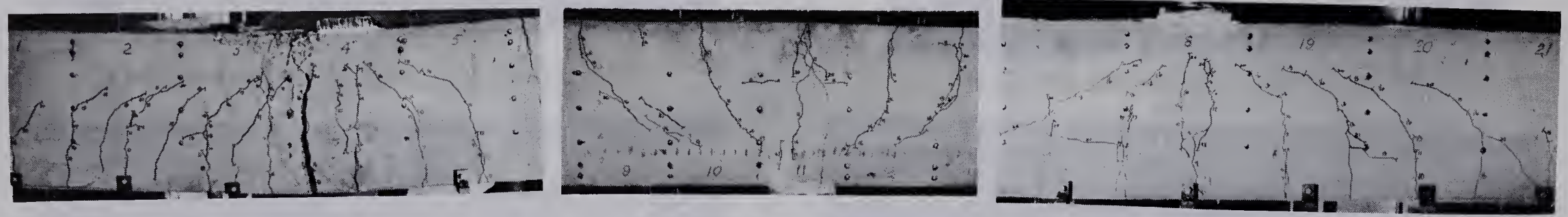

H.106

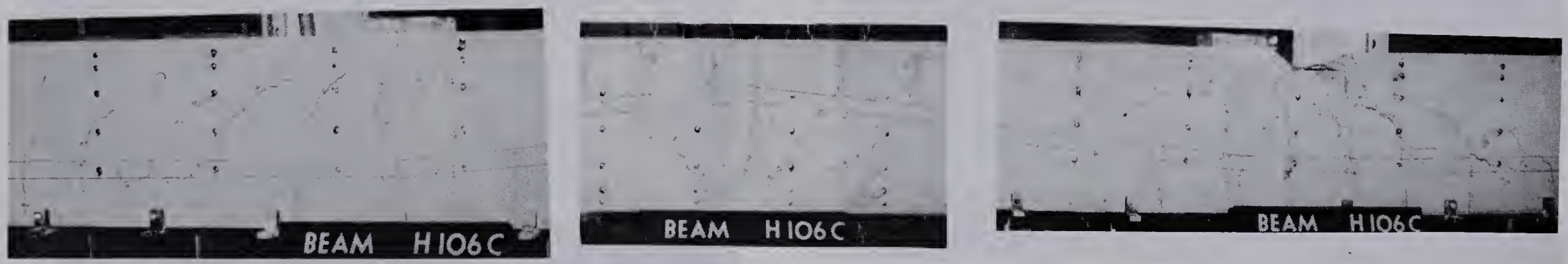

H.106.C

FIGURE 5.1 CRACK PATTERNS, SERIES 'H'

TENSION FAILURE WITH CRUSHING, H106

SPALLING AND SEVERE CRACKING, H108

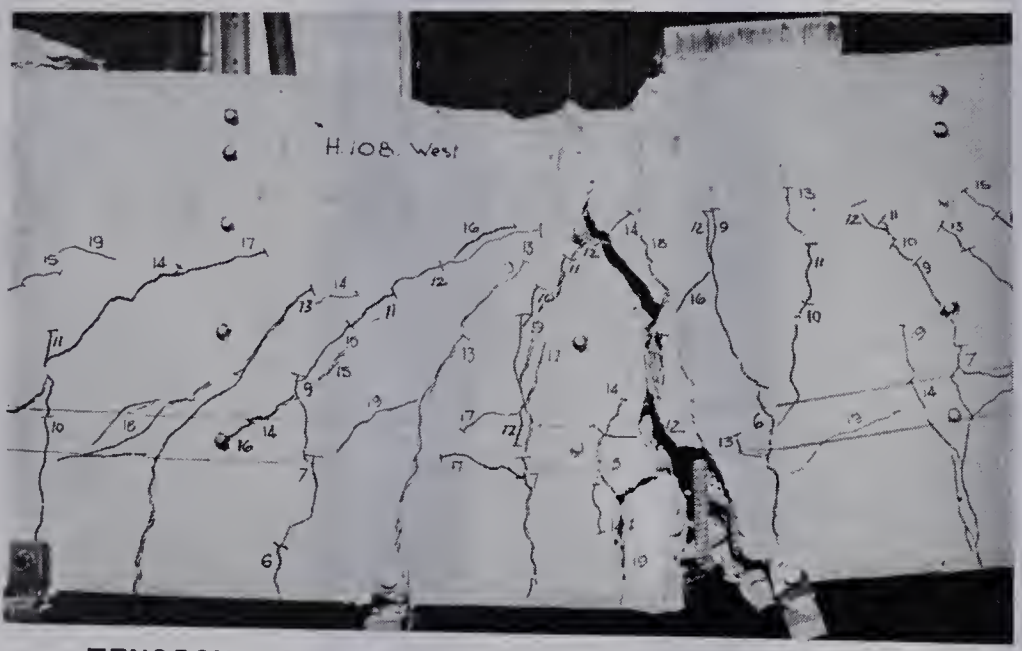

TENSION FAILURE AND SPALLING, H108

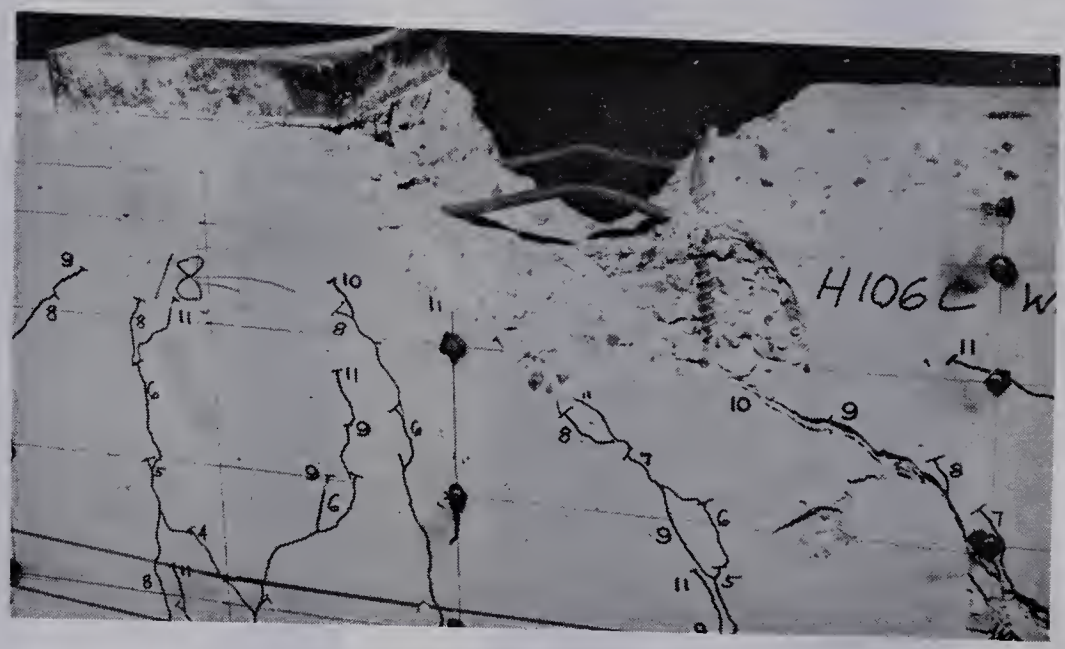

COMPRESSION FAILURE, H106.C

FIGURE 5.2 DETAILS OF FAILURE MODES, SERIES 'H'

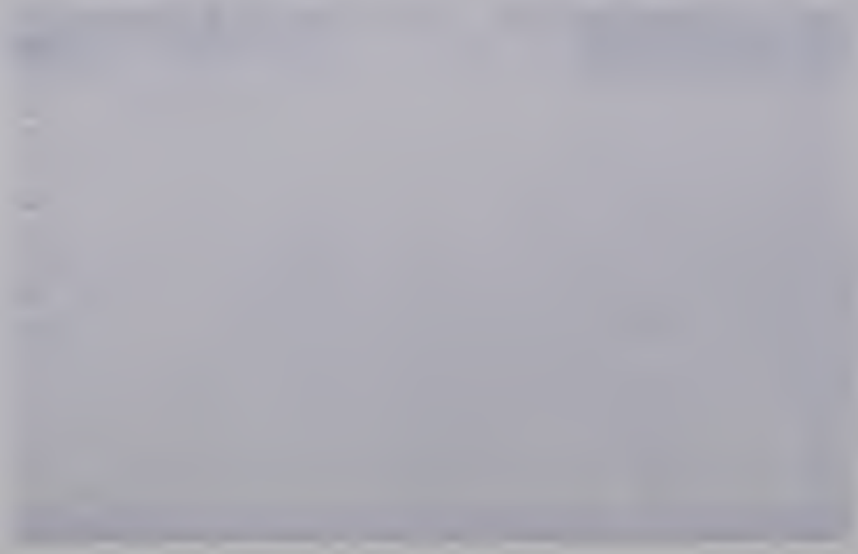

NORTH SOUTH

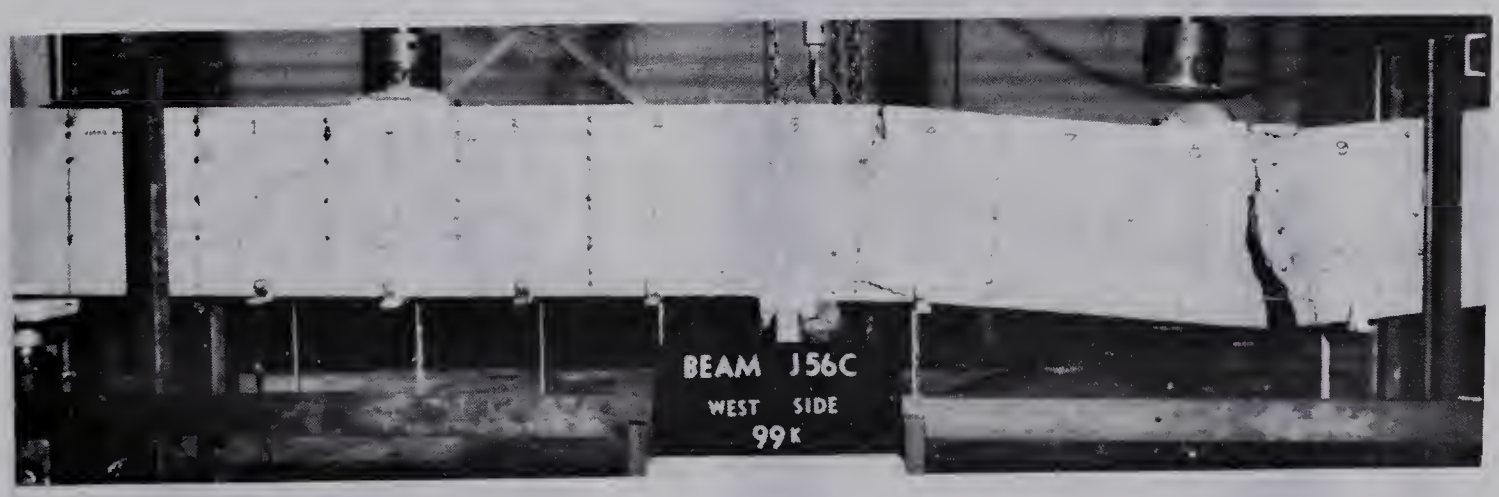

FIGURE 5.3 CRACK PATTERNS, SERIES 'J'

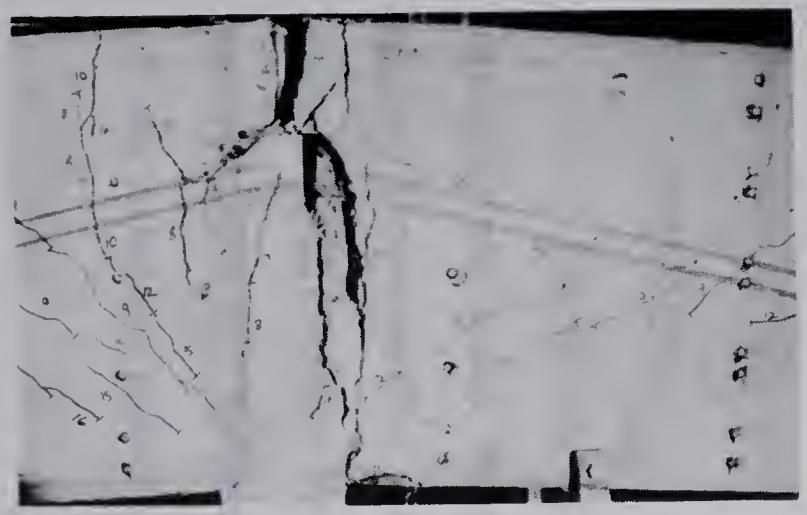

SECONDARY TENSION FAILURE, J58

SIMULTANEOUS TENSION FAILURES, J56

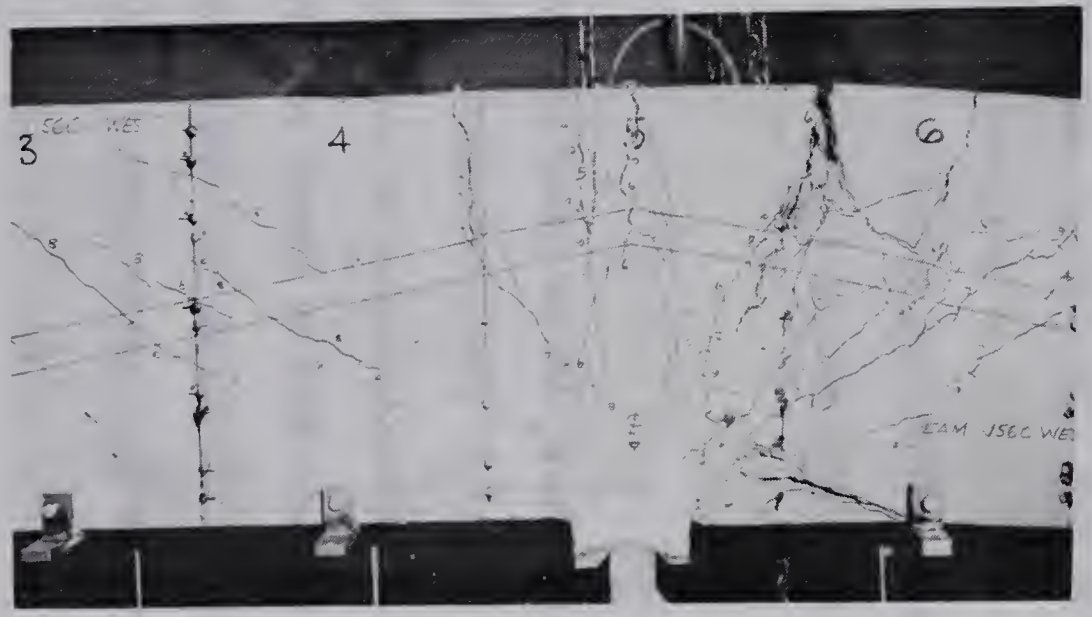

SPALLING AND SEVERE CRACKING, J56C

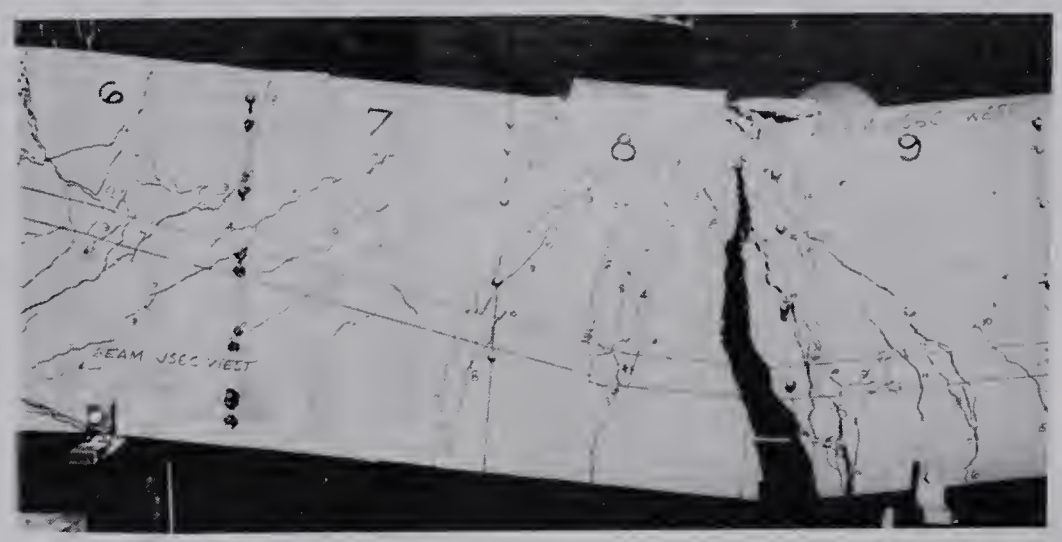

TENSION FAILURE WITH SPALLING, J56.C

FIGURE 5.4 DETAILS OF FAILURE MODES, SERIES 'J'

CHAPTER VI

SUMMARY

6.1 Summary

Six, two-span continuous prestressed concrete beams were tested in combined flexure and shear. Four of the beams included spiral confinement in the compression zones at the points of maximum moment. Their behaviour has been recorded in terms of applied loads and resulting deformations. Of particular interest was the effect of the confinement on the deformation capacity of the beams, and also whether continuous beams, reinforced in this way, were able to utilize any additional deformation capacity to form a true mechanism. The series also attempted to expose any difficulties which could be improved upon for future tests in the programme.

6.2 Conclusions

The following conclusions are based on the results of tests on six beams, each of which included different variables. The object of the series was not, therefore, to make any specific conclusions, but rather to investigate the trends of behaviour so that future tests may concentrate in more detail on particular aspects of the rotation capacity of continuous, prestressed concrete beams.

The conclusions may be summarized as follows:-

(a) Full moment redistribution is not likely to occur, or even required to occur, if the ratio of elastic to ultimate moments is near to 1.0.

(b) For a particular effective depth and prestress, the moment-curvature relationship over an interior support may be considerably different to that for a span section. This may be due to additional confining effects at the interior support resulting from a triaxial state of stress in the region of the supporting plate; it may also be due to differences in the strand profiles at the two sections.

(c) The presence of spiral confinement in no way affected the ultimate moment, or moment-curvature characteristics, of those beams whose reinforcement ratio was less than that specified by the A.C.I. Code, (Clause 2609).

(d) Shear reinforcement designed in accordance with the A.C.I. Code was adequate in preventing shear failures in all the continuous beams tested.

(e) Confinement provided by a 2" pitch spiral was effective in producing a relatively ductile failure in the two beams which would otherwise have failed in compression.

6.3 Recommendations

(a) The present test series was not sufficiently demanding on rotation capacity to expose the full limit of ductility. The elastic distribution of moments between positive and negative regions was too near to the ratio of ultimate moments, so that the plastic

rotation required to achieve a true mechanism was in no case critical. For the same reason, only once was full redistribution of moments achieved.

Since more demand on sections will be required in practice it is therefore recommended that future tests be designed so that the first hinge to form must deliver considerably more rotation before a mechanism is formed. This may be achieved by changing the loading system whilst keeping the ultimate moments constant at the hinges, or by providing a lower moment capacity at the first hinge to form than at the later hinges, or by a combination of both.

(b) A future extension of the investigation into continuous prestressed beams might usefully be concerned with I or T sections, although the latter are usually uneconomic in continuous structures. Confinement might be provided in these sections using a series of smaller diameter spirals.

(c) It is recommended that in future tests the control beams be those which are over-reinforced, since little difference was observed between the deformation characteristics of the #6 and #6.C beams in this series.

(d) Specifically, it is suggested that any future tests with continuous beams include a load-cell to measure the reaction at every support in order to provide a statical check. Although cross-checking of the calibration of the two load-cells used in this present series cancelled any doubts about measured moment distributions, it would have served as an assurance to have had a statical check.

(e) A further improvement in the testing method might be to adopt a direct rotation measuring device. This would serve firstly as a check on the integration of curvatures, and secondly to provide further information at loads approaching the ultimate for which mechanical strain-gage readings cannot be taken without risk to personnel.

(f) Future tests might concentrate on achieving more consistent values of concrete strength in order to reduce the variations in the series, thus providing a means for a better comparison.

REFERENCES

1. American Concrete Institute, "Building Code Requirements for Reinforced Concrete. (A.C.I. 318-63)", June, 1963.

2. Base, G.D., Read, J.B., "Effectiveness of Helical Binding in the Compression Zone of Concrete Beams", Journal, American Concrete Institute, July, 1965.

3. Ward, R.L., "Pretensioned Beams with Confined Compressed Concrete", M.Sc. Thesis, University of Alberta, April, 1966.

4. Wilkinson, M.K., Warwaruk, J., "Moment-Curvature Relationships of Prestressed Concrete Beams with Confined Compressed Concrete", Structural Engineering Report #17, University of Alberta, January, 1969.

5. Hawkins, N.M., Sozen, M.A., Siess, C.P., "Strength and Behaviour of Two-span Continuous Prestressed Concrete Beams", Structural Research Series #225, University of Illinois, September, 1961.

6. Mattock, A.H., "Rotational Capacity of Hinging Regions in Reinforced Concrete Beams", A.C.I. Symposium, "Flexural Mechanics of Reinforced Concrete", November, 1964, pp 143.

7. Corley, W.G., "Rotational capacity of reinforced concrete beams", Portland Cement Association, Development Department, Bulletin D. 108.

8. Blume, J.A., Newmark, N.M., Corning, L.H., "Design of Multistory Reinforced Concrete Buildings for Earthquake Motions", Portland Cement Association, 1961.

9. Warwaruk, J., Sozen, M.A., Siess, C.P., "Strength and Behaviour in Flexure of Prestressed Concrete Beams", University of Illinois, Experimental Station Bulletin #464, August, 1962.

NOTATION.

(unless otherwise defined in the text.)

A_s	Total area of prestressing strands.
d	Depth from extreme compression fibre to centre of gravity of prestressing strands.
f'_c	Mean concrete cylinder crushing strength.
f'_s	Ultimate strength of prestressing strand.
f_{su}	Stress in prestressing strand at failure.
L	Span length.
M_{cr}	Maximum moment at initial flexural cracking.
M_{sp}	Maximum moment at initial spalling.
M_u	Maximum moment corresponding to ultimate load.
P_e	Effective prestressing force.
p	A_s/bd; ratio of prestressing steel.
P	Applied load.
P_u	Applied load at failure.
$P_{sh.cr.}$	Applied load at initiation of shear cracks.
Z	Distance from points of maximum moment to zero moment.
Δ	Deflection.
θ	Rotation.
Ψ	Average curvature.

APPENDIX A

APPENDIX A

A.1 Materials

a) Cement

Type III, high-early strength, Portland cement was used in all mixes.

b) Aggregate

The sand had a fineness modulus of 2.53 and an average moisture content of about 4%. The coarse aggregate was a pea-gravel with a maximum size of 3/8". Sieve analyses for the sand and coarse aggregate are presented in Tables A.1 and A.2. Both aggregates have been used in this laboratory for several previous investigations and have passed the usual specification tests.

c) Concrete Mix

A satisfactory mix for this type of work had been developed by Wilkinson[4] using the same materials. The same mix design was adopted for this present test series. The ratios, by weight, per batch were:-

Cement	1.0	(170 lbs.)
Sand	2.2	(380 lbs.)
Coarse Aggregate	1.6	(270 lbs.)
Water	0.39 to 0.51	(67 to 87 lbs.)

The water/cement ratio was varied when necessary in order to attain a slump of at least 2½", and at the same time to maintain a strength of at least 5000 p.s.i. A workable mix was required because most of the beams were congested with reinforcement, and compaction would have been difficult had a stiffer mix been used.

Concrete cylinder strengths varying from 4600 to 6110 p.s.i. were obtained, each value representing the average of three cylinder strengths per batch. The overall coefficient of variation for all batches was 9.8%. The properties of the concrete batches, and the cylinder results, are presented in Table A.3.

d) Prestressing strand

The prestressing strand used for the test beams was 250K. grade, 7-wire strand, with 5/16" nominal diameter, and complied with ASTM-A-416 Specifications. The stress-strain diagram, as supplied by the Manufacturers, is shown in Figure A.1.

e) Shear reinforcement

The stirrups were made up from either #2 plain bars or #3 deformed bars. The yield strengths were 42 k.s.i. and 55 k.s.i. respectively.

f) Spiral reinforcement

All the spiral reinforcement was fabricated using #2 plain bars, with a yield strength of 42 k.s.i.

A.2 Fabrication

a) Formwork

The forms were fabricated in three sections, each 8 ft. long.

The forms were made of plastic-coated, ½" plywood stiffened with timber battens to maintain the beam shape under the pressure of the newly cast concrete. In order to accommodate the holding-down system beneath the base form, the whole length of form was supported on 6" deep joist sections to which clamping devices were fixed to hold the sides in place.

b) Prestressing operation

The prefabricated shear cages were laid on the base of the formwork with the sides removed to provide accessibility. The pre-stressing strands were threaded through the steel formers at the ends of the beam, and through the three specially machined steel blocks which were to be left in the beam. At one end of the beam, each strand was threaded through an aluminum dynamometer and gripped in a C.C.L. anchoring device, as illustrated in Figure A.2. At the other end of the beam, the strands were similarly prepared for tensioning. The level of the centre of gravity of the strands was checked and adjusted when necessary by means of the locking nuts on the three steel blocks.

With the strands in position, they were jacked horizontally to a calculated level less than the required initial prestress. Each strand was tensioned individually using a Simplex centre hole hydraulic jack operated by an electrically driven, Blackhawk hydraulic pump. The additional stress required in the final position was achieved by jack-ing vertically, to the required eccentricity, at the centre of the beam. This operation is also illustrated in Figure A.2. At this stage, read-ings were taken of the electrical strain gages attached to the aluminum dynamometers and to the vertical load cell above the jacking frame, from which the loads were derived. If necessary, the whole system could be released and the process repeated until the required tensions

in the strands were produced. When a set of satisfactory readings was achieved, the locking nut above the load cell was tightened to transfer the load from the vertical jacks to the frame, and the jacks were removed. With the strands in their final profile, the spirals were placed in position and all the supplementary reinforcement was tied securely to the strands. The sides of the formwork were erected and adjusted for alignment, and the concrete was cast.

c) Casting and curing

The concrete was mixed in a nine cubic feet capacity, vertical drum mixer. Series 'H' beams required three batches, each of about six cubic feet, to cast the beam and its control cylinders. Series 'J' beams each required two of the same batches. The concrete was compacted using an immersion type vibrator. Beam J58, which was particularly congested, required that a supplementary external vibrator be used.

For each batch of concrete, five 6" x 12" control cylinders were cast; three of these were tested in compression and the remaining two in splitting.

Immediately after casting, each beam was enclosed in saturated burlap which was then covered by a damp-proof sheet, in an attempt to minimize early shrinkage cracking, and to promote curing. The side forms were stripped after twenty-four hours, and the atmosphere was maintained humid for the five days prior to release by keeping the burlap wet. After release, the beams were stored in the laboratory atmosphere. The control cylinders were always subjected to the same curing conditions as the beams.

d) Release of prestress

The prestress was released, in all beams, five days after casting. The first stage in the procedure was to cut the strands at one end of the beam. This was achieved by gently applying heat from an oxy-acetylene flame, over a length of about three feet between the stop-end and the bulkhead, until the individual strands broke. The fracture was always quite gentle, indicating that a steady transfer of stress into the concrete had occurred. By releasing the prestress in this way, the loads in the holding-up and holding-down systems were reduced to practically zero, and these were then released.

A set of mechanical strain gage readings was taken before and after release in order to determine the elastic losses.

A.3 Prestress losses

The interior support and mid-span sections were treated separately from the point of view of prestress losses.

A complete set of mechanical strain gage readings was taken immediately before and after release, and these were used, together with the initial readings taken at the start of each test, in order to calculate losses of strain.

Losses which occurred during the prestressing operation due to anchorage slip and to release of the horizontal jack, all took place before the initial prestress was calculated. Therefore the losses which are presented under the "Total loss" heading in Table A.4 refer to elastic, creep and shrinkage losses in the concrete, and to any relaxation loss in the steel.

4.1 Balance of Learning

The framework was released, in all honesty, from any exter-
nalities. The first stage in the framework was to find the balance at
end-of the game. This is achieved by gently exploring each area as
the-destiny-time flows over a longer of every game that balances the stan-
ard and the economy with the behavioural strength areas. The Inventory
was always quite pretty, including that a theory-fiction of visual
ing the contents the account. It removing the treatment in his way,
the level is the defining of the activity-core systems with respect to
practically even, and that's more the system.

I bet it before in every game teaching was take action
and after release to speak to economy the ability level.

4.2 Exploring Level

The exercise looping and pre-game setting more tension
especially from the point of exercise, cause.

A quality all of mechanical create game teaching was cause
necessary before the other actions, and there may avoid capacity
with the initial sessions level at the start of each year, to ensure
to structure formal of level.

Level play economy during the practicing question the
to behaviour effected to balance of the successful back, all that cause
option the initial dynamic and mechanics. Therefore the level
which are economic player are "core loop" leading to close E.G game
to attack, when and difficult issues in the economy, and on any
practice loop in the level.

The initial prestresses in the horizontal strands were calculated from the dynamometer readings taken immediately before release. The initial prestresses in the sloping strands were calculated from the readings of the vertical load cell, and these were found to compare favourably with the predicted values. The horizontal components of the initial prestresses are presented in Table A.4.

The changes in strain distribution, both immediately after release and before testing, were plotted and the change in strain at the level of the prestressing strands was calculated. For the end sections the average of the six end gage lengths was used, and for the interior section the average of the three central gages was used. Prestress losses and effective prestress levels are also recorded in Table A.4.

A.4 Loading apparatus

The two concentrated loads were applied at the mid-spans by means of two 220 kip. Amsler hydraulic jacks. The loading frame and jack arrangement are shown in Figure A.3, as set up for the longer span beams. An Amsler pendulum dynamometer formed an integral part of the loading system, and was used to measure the applied loads. Equal loading at the two points was assured by coupling the hydraulic jacks in parallel. A load maintainer made it possible to keep the applied loads at a constant level, independent of rapidly increasing deflections in the beam. However, this arrangement did not facilitate an accurate observation of the beam behaviour immediately prior to collapse since such a system is inherently unstiff.

The loads were applied through 6" x 6" steel bearing plates which were plastered to the top of the beam. Similar plates were provided at the three reaction points, though later, for series 'J' beams, a 4" x 6" plate was used at the interior support. All three supports were hinged so as to permit rotation, and the two external supports included roller bearings, as shown in Figure A.4, to allow horizontal freedom.

TABLE A.1

SIEVE ANALYSIS OF SAND

Sieve Size	Weight Retained (gms)	% Retained	Cumulative % Retained	A.S.T.M. Standard
#4	17.5	3.0	3.0	0 - 5
#8	85.2	14.7	17.7	-
#16	54.6	9.5	27.2	20 - 55
#30	60.0	10.3	37.5	-
#50	208.4	35.8	73.3	70 - 90
#100	122.9	21.1	94.4	90 - 98
Pan	17.8	3.1	-	-
Silt	14.4	2.5	-	-
Total	580.8	100.0		
Fineness Modulus		2.53		

TABLE A.2

SIEVE ANALYSIS OF COARSE AGGREGATE

Sieve Size	% Retained	Cumulative % Retained
3/4	0	0
3/8	5.9	5.9
#4	87.1	93.0
Pan	7.0	100.0
Total	100.0	

TABLE A.3

CONCRETE PROPERTIES AND CYLINDER RESULTS

BEAM	BATCH	W/C (by weight)	SLUMP (inches)	AGE AT TEST (days)	AVGE. CYL. STRENGTH	AVGE. SPLITTING STRENGTH	COEFF. OF VARIATION
	1	0.51	2 3/4		4960	441	
H108	2	0.51	2 1/2	41	5160	400	4.3%
	3	0.51	2 3/4		5140	514	
	1	0.46	2 1/2		5960	461	
H106	2	0.47	2 1/2	36	5640	388	8.5%
	3	0.50	3		5820	421	
	1	0.50	3 1/4		4600	364	
H106.C	2	0.51	2 1/2	47	5440	457	10.4%
	3	0.51	2 1/2		5560	407	
	1	0.46	2 1/2		5670	412	
J58	2	0.50	2 1/2	18	6110	508	6.3%
	1	0.43	2 1/2		6060	444	
J56	2	0.49	2 3/4	17	5330	424	12.1%
	1	0.42	2 1/4		5700	456	
J56.C	2	0.39	2 1/2	17	5300	434	4.8%

TABLE A.4

A SUMMARY OF THE PRESTRESS LOSSES

	(SPANS)				(INTERIOR)		
BEAM	INITIAL PRESTRESS (k.s.i.)	ELASTIC LOSS %	TOTAL LOSS %	P_e (k.s.i.)	INITIAL PRESTRESS (k.s.i.)	TOTAL LOSS	P_e (k.s.i.)
H108	149	6.9	16.7	124	147	17.3	122
H106	141	5.5	14.3	121	136	14.5	116
H106.C	144	4.6	16.7	120	142	16.3	119
J58	158	5.4	10.5	141	147	10.2	132
J56	168	4.3	10.2	151	158	9.7	143
J56.C	159	3.8	10.4	143	153	10.1	138

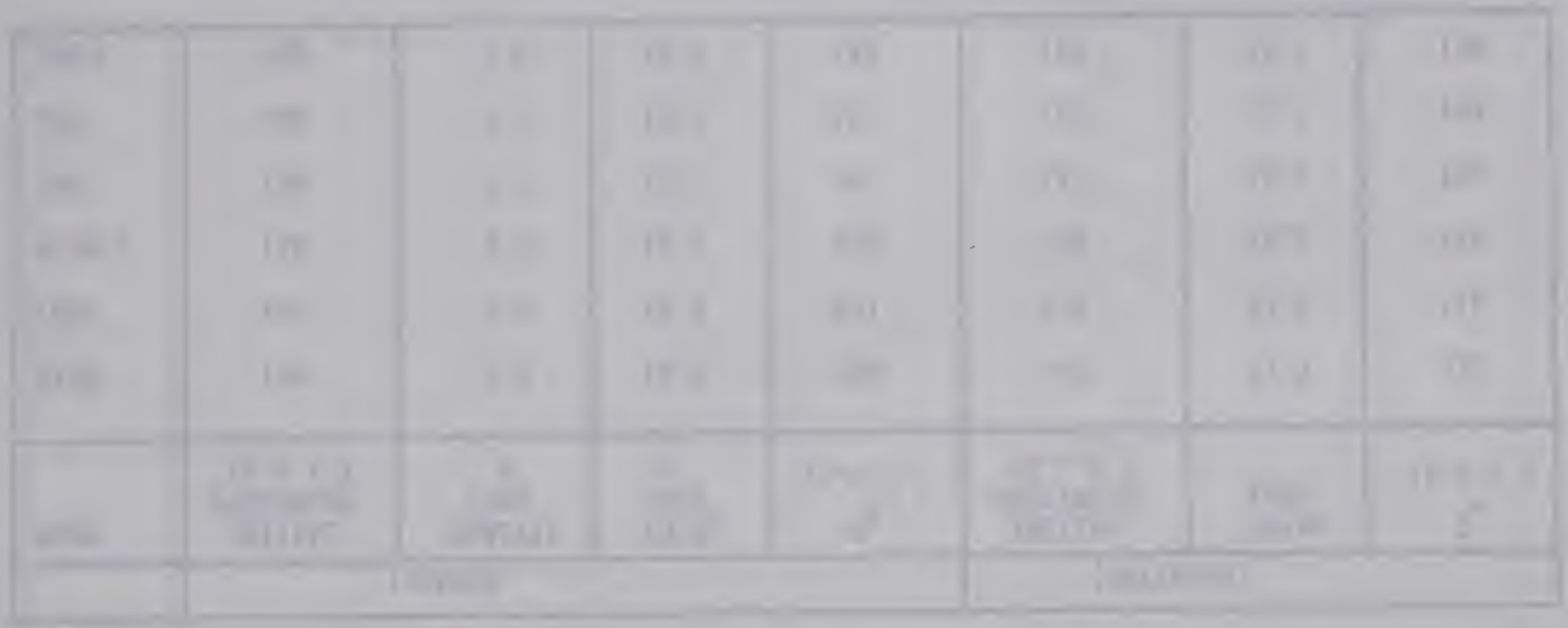

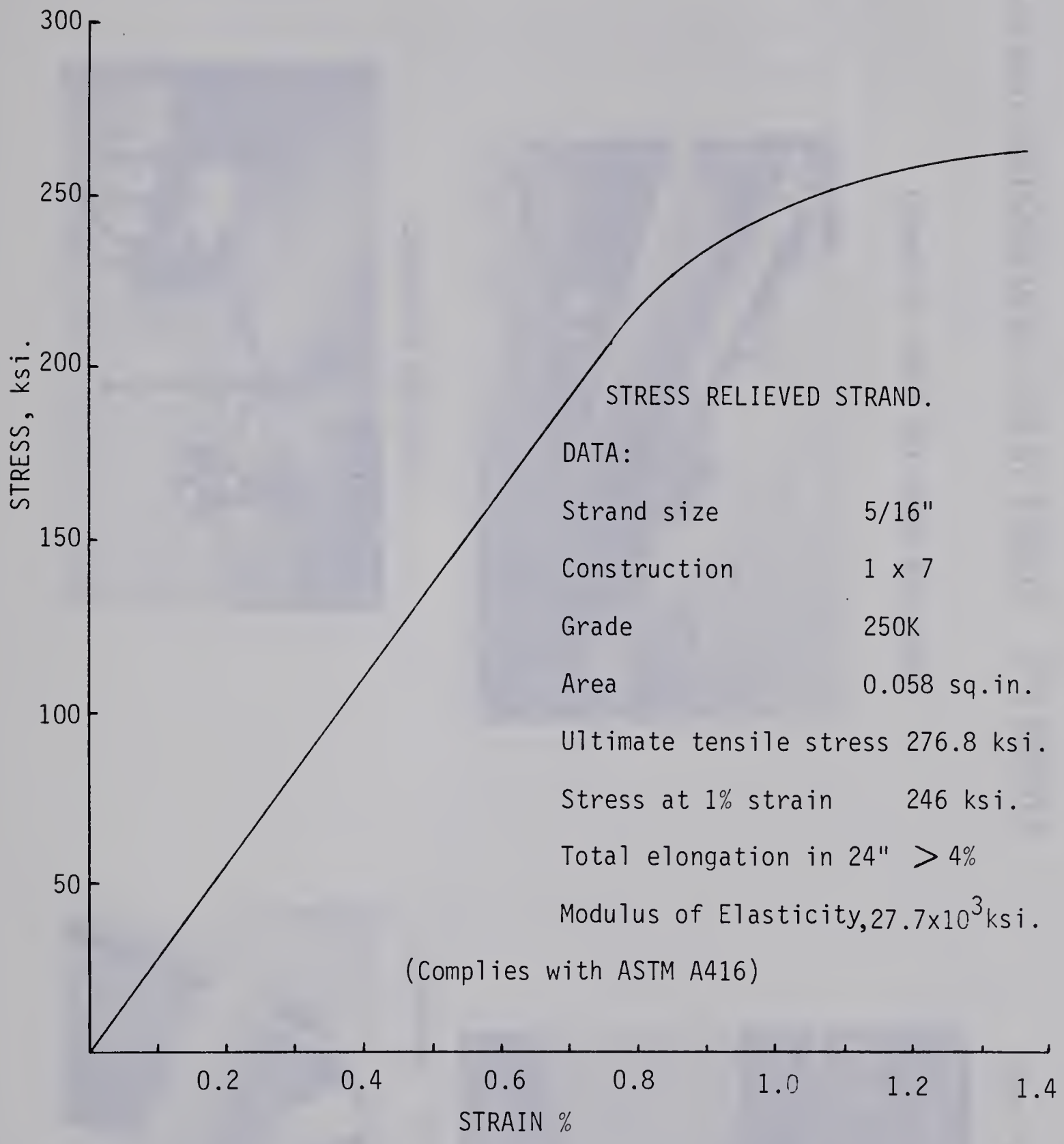

FIGURE A.I STRESS-STRAIN RELATIONSHIP FOR PRESTRESSING STRAND

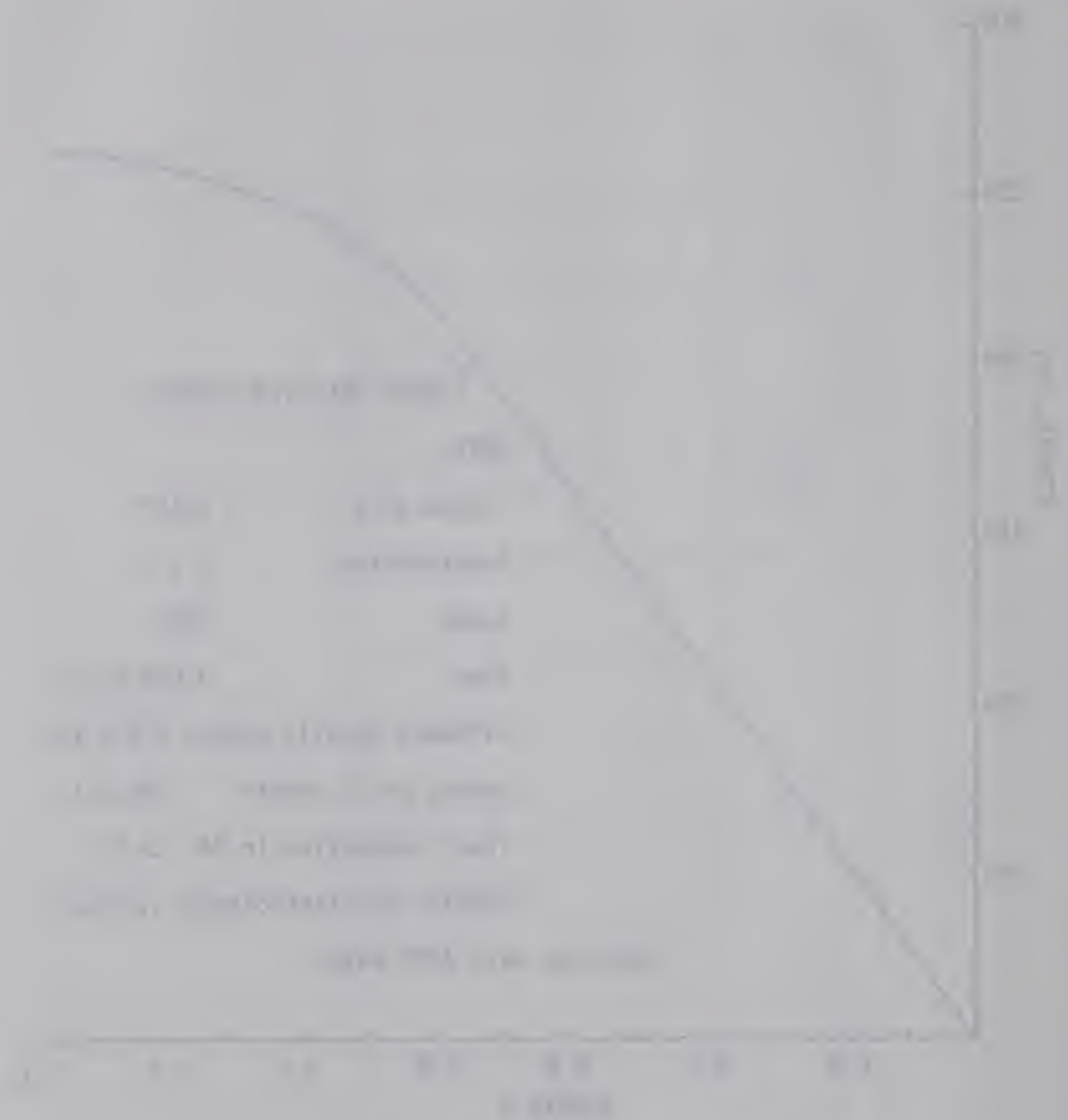

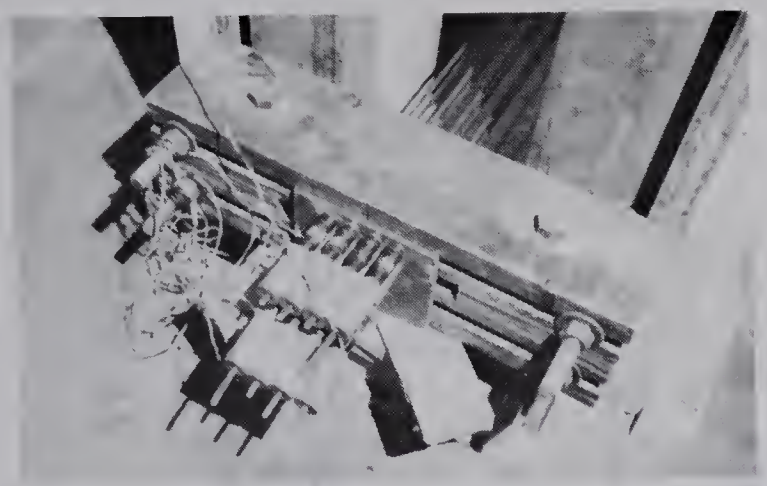

DYNAMOMETERS AND CCL. ANCHORAGES

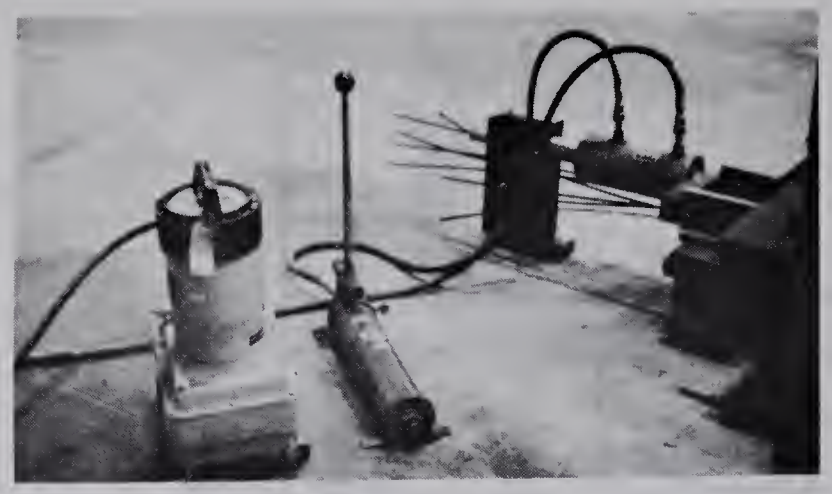

JACKING EQUIPMENT

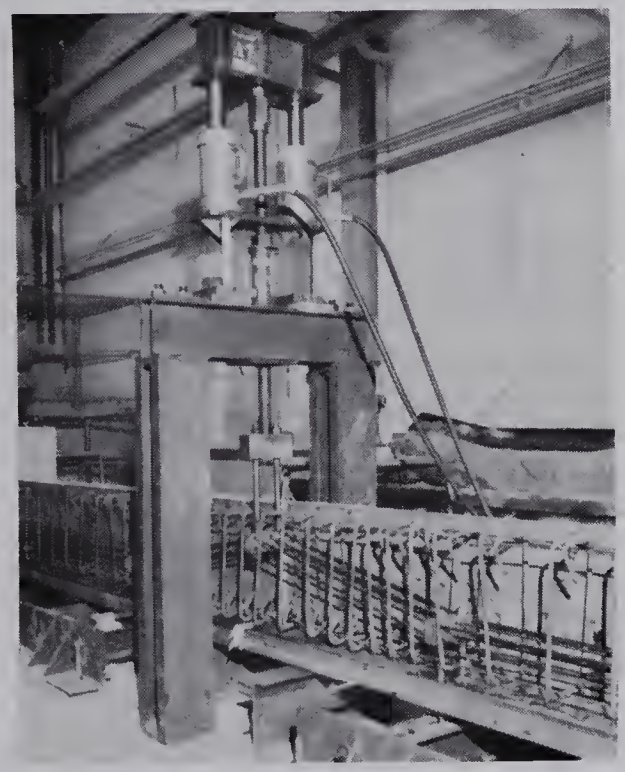

JACKING VERTICALLY, J56.

BEAM H108 READY FOR FINAL ALIGNMENT

FIGURE A.2 STAGES IN THE PRESTRESSING OPERATION

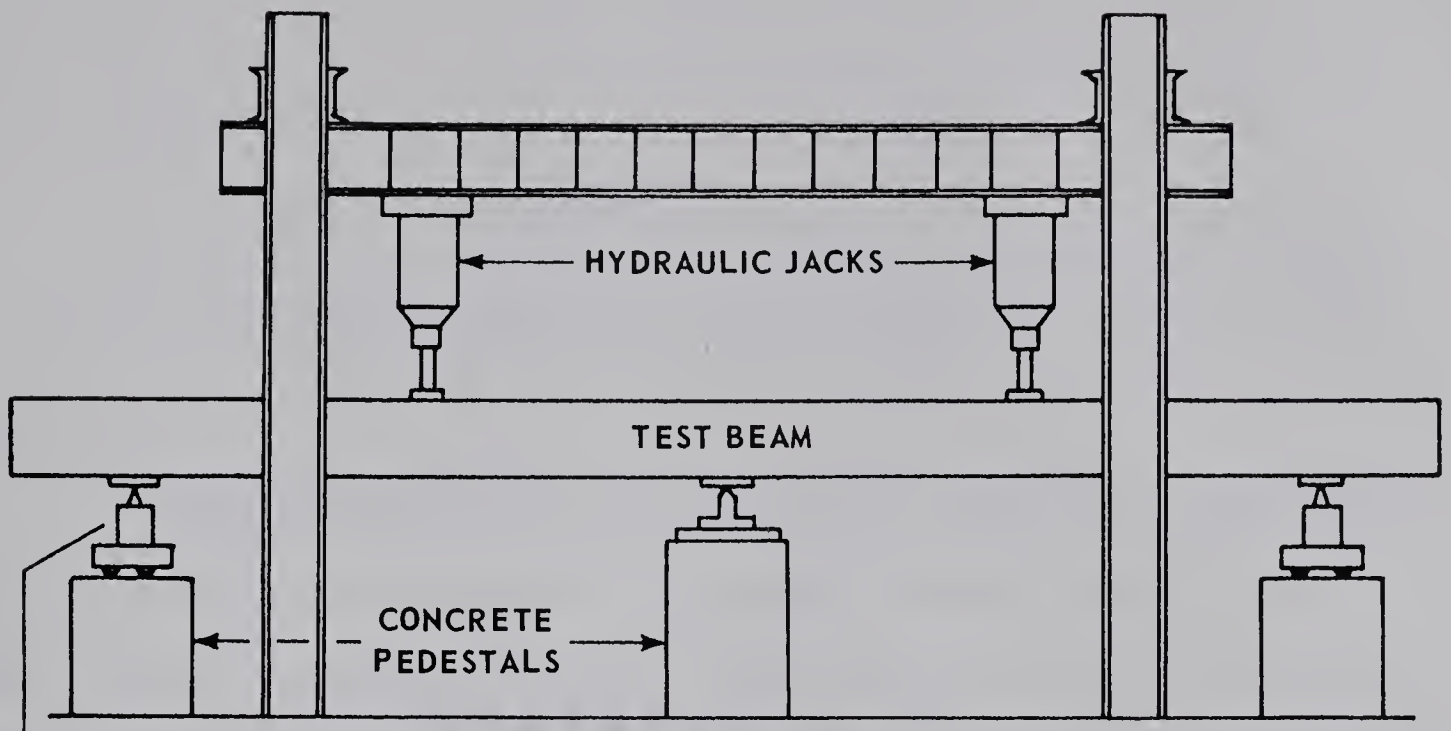

FIGURE A3 LOADING FRAME

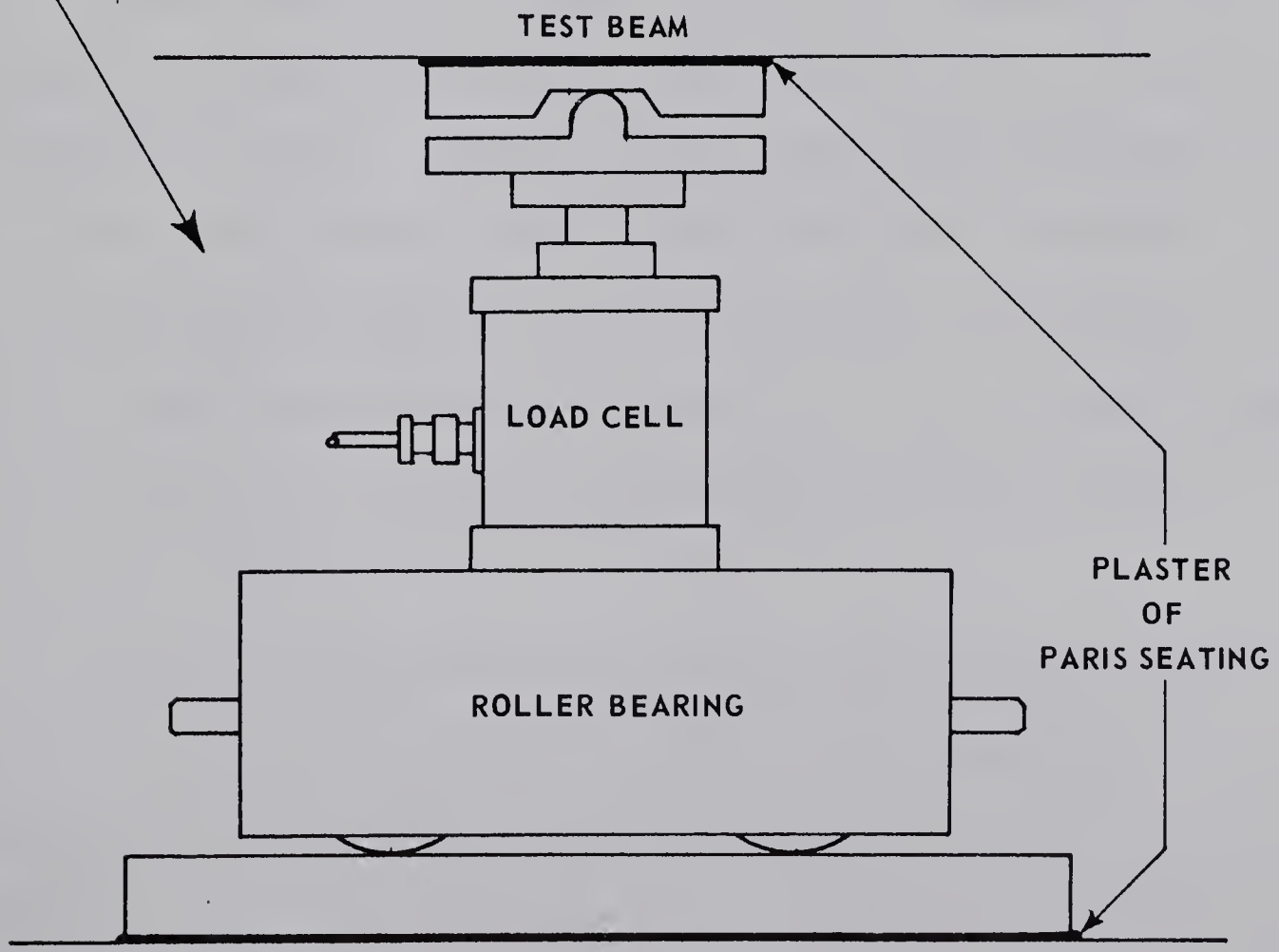

FIGURE A4 DETAIL OF AN EXTERIOR SUPPORT

APPENDIX B

APPENDIX B

CORRELATION OF RESULTS WITH THEORY

Any theoretical solution for a moment-curvature relationship requires that the stress-strain relationship for the material be defined. Blume, Newmark and Corning[8] have developed such a relationship for bound concrete; it is shown in Figure B1, in terms of the section parameters.

The derivation of the complete theoretical moment-curvature plot, using the assumed stress-strain relationship, would be possible using a digital computer. However, in this case, only the ultimate moment and curvature for each failure section have been calculated.

For those sections with spiral confinement, failure was defined at either the curvature corresponding to a steel strain of 0.04, or that corresponding to an extreme-fibre concrete strain of 0.01, whichever was the smaller.

To find the compatible strains corresponding to equilibrium of internal forces, a step-by-step programme was written which took into account the effect of crushing of the concrete by ignoring its contribution to the compressive force, and using only that concrete confined by the spiral.

For those sections without confinement, the concrete strain corresponding to failure was taken as 0.004. The approach used to

calculate the ultimate moments and curvatures for these sections was that presented by Warwaruk[9].

For each beam, the values of concrete strength and effective prestress used in the calculations were those determined from the test results, as presented in Table 3.1.

The results of the calculations are presented in Table B1.

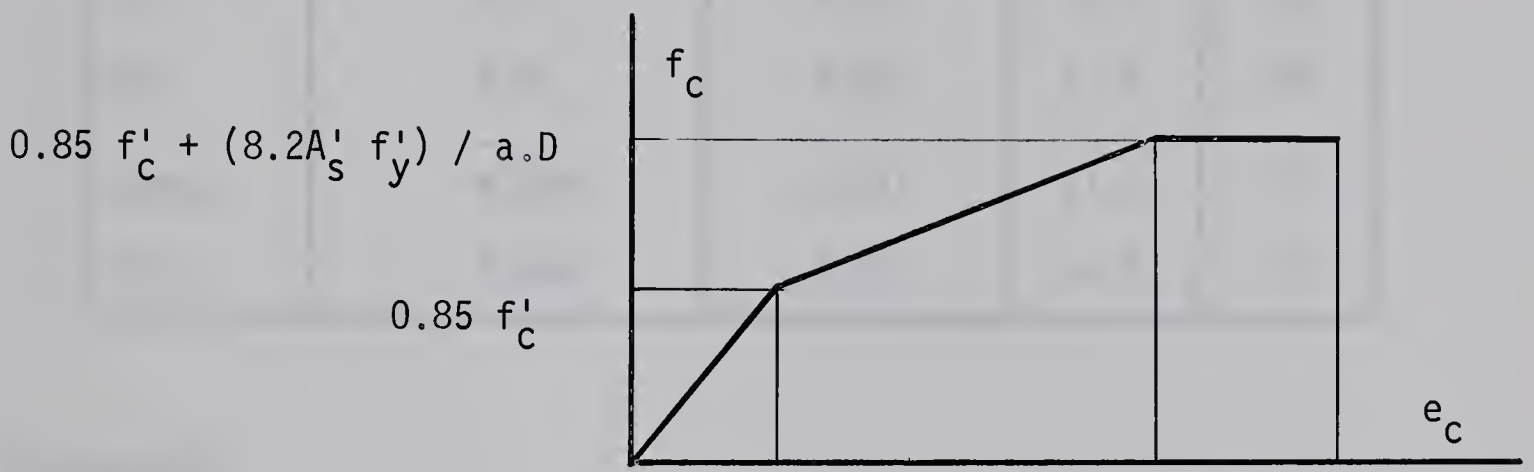

FIGURE B.1 Assumed Stress-Strain Relationship for Bound Concrete[8]

DATA:-

- f'_c - concrete cylinder strength
- A'_s - cross-sectional area of spiral reinforcement - 0.047 sq.in.
- f'_y - yield stress of spiral reinforcement - 40 ksi.
- a - pitch of spirals - 1" or 2"
- D - diameter of spirals - 6"
- e'_y - yield strain of spiral reinforcement - 0.0016
- e'_{su} - ultimate strain of spiral reinforcement - (>0.002)

TABLE B1

RESULTS OF THEORETICAL ANALYSIS

Beam	Concrete Strain at Failure	Steel Strain at Failure	M_u (K.ft.)	ψ_u (in^{-1})
H108	0.01	0.013	73.8	185
H106	0.01	0.021	60.9	263
J58	0.01	0.015	76.1	200
J56	0.01	0.023	61.3	270
H106.C	0.004	0.011	61.0	101
J56.C	0.004	0.013	65.0	111

Discussion

It has been assumed that the ultimate curvature is determined when a limiting strain is reached, either in the steel or the concrete. In terms of theory, both of these are essentially arbitrary. The results, in Table B1, indicate that in all cases a strain of 0.01 in the concrete determined the ultimate curvature. Corresponding to this strain, the strain in the steel is seen to vary from 0.013 to 0.023. The steel strain represents an average value, and not necessarily a maximum value which would correspond with the location of a crack. Therefore, whilst it is unlikely that a maximum steel strain in excess of 0.04 would correspond to an average steel strain of 0.013, it cannot be certain that limiting steel strains would not occur before limiting concrete strains.

Tension failures occurred in all the test beams, indicating that in fact a limiting steel strain was critical in determining failure. However, it was not possible to determine the magnitude of the strain in the steel at failure, and so further correlation is not meaningful.

APPENDIX C

APPENDIX C

ESTIMATION OF ULTIMATE CURVATURES - CALCULATIONS

Mattock[6] has proposed that a measure of the total inelastic rotation, occurring between points of maximum moment and zero moment, may be obtained from the measured maximum (mid-span) deflections. He assumed that the mid-span deflection could be divided into a component due to elastic deformation and a component due to inelastic, or plastic, deformation. The plastic deformation is assumed to be concentrated at the point of maximum moment, and is equal to $\Delta_p/(L/2)$, where L is the span and Δ_p is the inelastic component of deflection. Although this is not an exact measure of the total inelastic rotation occurring in the length Z, Mattock believes that it is a measure of the total inelastic rotation, suitable for use in theories of limit design.

On this basis, the inelastic rotations were calculated. However, a modification was made. Table 5.3 presents the ratio of the total rotation which occurred in the length d/2 to one side of a hinge, in terms of the total rotation occurring in the shear span, Z. Using this ratio, then, it was possible to be more precise about the rotation occurring in d/2, and hence, combining the ratios on each side of a hinge, to obtain the rotation occurring over the 10" gage length, which happened to be equal to d, the effective depth of the beams.

The first stage was to calculate the inelastic rotation, at the penultimate load, occurring in 10", being a ratio of the total inelastic rotation occurring in two adjacent shear spans (zones 1 and 2 in Table 5.3). Dividing this rotation by 10 gave the average curvature over the 10" gage length, which, when added to the estimated elastic curvature (from Figures 4.4 and 4.5) gave the total average curvature. A test of the validity of this approach was provided by comparing the curvatures obtained by this method with those obtained from the strain readings at the penultimate load, (see Table 5.4). To estimate the ultimate curvature, it was assumed that the rotation occurring over the final load increment was confined to the central 10" gage length, and that there was no increase in rotation outside this zone. The change in inelastic rotation was calculated from the change in deflection in a similar manner as for the penultimate load. When added to the inelastic rotation at penultimate, the result was the total ultimate inelastic rotation. By dividing by 10, the average inelastic curvature over the 10" gage lengths was calculated, and this, when added to the elastic curvature gave the final (average) total curvature over the 10" gage length.

In terms of symbols:

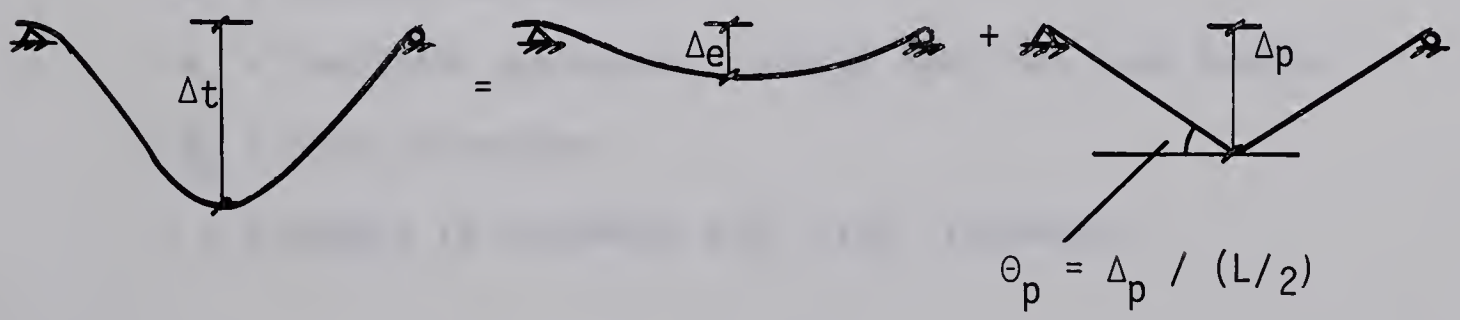

At penultimate load:-

$$\theta'_{p(Z)} = \frac{\Delta'_p}{(L/2)}$$

$$\theta'_{p(10)} = (r_1 + r_2).\theta'_{p(Z)}$$

$$\psi'_{p(10)} = \frac{\theta'_{p(10)}}{10}$$

$$\psi'_{t(10)} = \psi'_{p(10)} + \psi_e$$

At ultimate load:-

$$\delta(\theta_{p(Z)}) = \tfrac{1}{2}.\delta(\theta_{p(10)}) = \frac{\delta(\Delta_p)}{(L/2)}$$

$$\delta(\theta_{p(10)}) = \frac{2.\delta(\Delta_p)}{L/2}$$

$$\theta_{p(10)} = \theta'_{p(10)} + \frac{2.\delta(\Delta_p)}{(L/2)}$$

$$\psi_{p(10)} = \frac{\theta_{p(10)}}{10}$$

$$\psi_{t(10)} = \psi_{p(10)} + \psi_e$$

Where:-

Δ_p = inelastic deflection

(fn') = parameter at penultimate load

(fn) = parameter at ultimate load

θ_p = inelastic rotation

ψ_e = elastic curvature

ψ_p = inelastic curvature (average over 10" gage length)

ψ_t = total curvature

δ = change in parameter over final increment

Example of calculation for Beam H108.

Δ'_p = 1.10"

L/2 = 60"

$\theta'_{p(Z)}$ = 0.0184 rad.

r_1 = 0.37

r_2 = 0.58

$\theta'_{p(10)}$ = 0.0175 rad.

$\psi'_{p(10)}$ = 0.00175 rad./in.

ψ_e = 0.00025 rad./in.

$\psi'_{t(10)}$ = 0.00200 rad./in. **

$\delta(\Delta_p)$ = 1.29"

$\delta(\theta_{p(Z)})$ = 0.0214 rad.

$\delta(\theta_{p(10)})$ = 0.0428 rad.

$\theta_{p(10)}$ = 0.0603 rad.

$\psi_{p(10)}$ = 0.00603 rad./in.

$\psi_{t(10)}$ = 0.00628 rad./in.

** Compare with curvature derived from strain distribution

= 0.00169 rad./in.